Human papillomavirus oncoproteins induce a reorganization of epithelial-associated γδ T cells promoting tumor formation

Dorien Van hede[a,b,c], Barbara Polese[d], Chantal Humblet[a], Anneke Wilharm[e], Virginie Renoux[a], Estelle Dortu[f], Laurence de Leval[g], Philippe Delvenne[f], Christophe J. Desmet[a], Fabrice Bureau[a], David Vermijlen[b,c,1,2], and Nathalie Jacobs[a,1,2]

[a]Laboratory of Cellular and Molecular Immunology, GIGA Research, University of Liège, 4000 Liège, Belgium; [b]Department of Pharmacotherapy and Pharmaceutics, Université Libre de Bruxelles (ULB), 1050 Bruxelles, Belgium; [c]Institute for Medical Immunology, ULB, 6041 Gosselies, Belgium; [d]Laboratory of Immunoendocrinology, GIGA Research, University of Liège, 4000 Liège, Belgium; [e]Institute of Immunology, Hannover Medical School, 30625 Hannover, Germany; [f]Experimental Pathology, GIGA Research, University of Liège, 4000 Liège, Belgium; and [g]Pathologie Clinique, Institut Universitaire de Pathologie, CH-1011 Lausanne, Switzerland

Edited by Willi K. Born, National Jewish Health, Denver, CO, and accepted by Editorial Board Member Philippa Marrack September 19, 2017 (received for review July 21, 2017)

It has been shown that γδ T cells protect against the formation of squamous cell carcinoma (SCC) in several models. However, the role of γδ T cells in human papillomavirus (HPV)-associated uterine cervical SCC, the third-leading cause of death by cancer in women, is unknown. Here, we investigated the impact of γδ T cells in a transgenic mouse model of carcinogenesis induced by HPV16 oncoproteins. Surprisingly, γδ T cells promoted the development of HPV16 oncoprotein-induced lesions. HPV16 oncoproteins induced a decrease in epidermal Skint1 expression and the associated antitumor Vγ5$^+$ γδ T cells, which were replaced by γδ T-cell subsets (mainly Vγ6$^+$ γδ^{low}CCR2$^+$CCR6$^-$) actively producing IL-17A. Consistent with a proangiogenic role, γδ T cells promoted the formation of blood vessels in the dermis underlying the HPV-induced lesions. In human cervical biopsies, IL-17A$^+$ γδ T cells could only be observed at the cancer stage (SCC), where HPV oncoproteins are highly expressed, supporting the clinical relevance of our observations in mice. Overall, our results suggest that HPV16 oncoproteins induce a reorganization of the local epithelial-associated γδ T-cell subpopulations, thereby promoting angiogenesis and cancer development.

γδ T cells | viral oncogene | interleukin 17 | functional heterogeneity | gammadelta

T cells bearing a γδ T-cell receptor (TCR) are unconventional T cells that display adaptive features such as the formation of a TCR by somatic recombination (like in αβ T cells) along with innate characteristics, such as a rapid response independent of professional antigen-presenting cells (1, 2). γδ T cells contribute to immune responses to infection, cellular transformation and tissue damage (2, 3). γδ T cells have well-established protective roles in cancer, largely on the basis of their potent cytotoxicity and IFN-γ production (3). Multiple studies in several mouse cancer models have established the protective role of γδ T cells during tumor development by comparing tumor progression in γδ T-cell–deficient mice (via genetic inactivation of the TCRδ locus) (4) versus γδ T-cell–sufficient mice [wild type (WT)] (5–8). In this regard, γδ T cells protect against the development of squamous cell carcinoma (SCC) (5, 9) and against transplanted B16 melanoma (6, 10). In line with these observations in mouse models, a recent study analyzing the gene expression profiles of thousands of samples derived from 39 different cancer types, including melanoma, revealed γδ T cells as the most significant favorable prognostic immune population (11). Tumor cell recognition and associated γδ T-cell activation have been attributed to engagement of the TCR and/or natural killer receptors (NKRs), mostly NKG2D (3). NKG2D is a crucial innate receptor in tumor surveillance, as demonstrated by the high cancer susceptibility of NKG2D-deficient mice. NKG2D is a sensor for molecular stress signatures [such as the NKG2D ligand retinoic acid early inducible 1 (Rae1) in mice] that are largely absent from healthy cells but often up-regulated by transformed cells (3).

In contrast to αβ T cells, γδ T cells are divided into subsets based on the type of γ and/or δ chain they express within their TCR, which are usually associated with particular organs and even particular tissue locations within these organs. Thus, the murine skin Vγ5Vδ1 T cells, also known as dendritic epidermal T cells (DETCs), are highly prevalent in the epidermis as intraepithelial lymphocytes, while other subsets (expressing the Vγ4 or Vγ6 chain) are enriched in the dermis (2, 12–15). The DETC TCRs are constitutively clustered and functionally activated in vivo at steady state, forming true immunological synapses that polarize and anchor T-cell projections at squamous keratinocyte tight junctions (16). It has been shown that Skint1, a member of the butyrophilin-like (Btnl) family of proteins that is selectively expressed by keratinocytes in the epidermis, drives the selective maturation of DETC progenitors. DETC are >90% ablated in Skint1 mutant mice, while all other T-cell populations are unaffected (17–19). More recently, a similar mechanism has been revealed for the intraepithelial γδ T-cell repertoire of the gut, both in mouse and human (20). Thus, the usage

Significance

Of all tumor-infiltrating leukocytes, T cells bearing γδ T-cell receptors have been associated with the most favorable prognosis. However, we show here, in a mouse model of carcinogenesis induced by human papillomavirus (HPV) oncoproteins, that γδ T cells promoted the development of HPV-induced lesions. Indeed, HPV-oncoprotein expression induced an infiltration of γδ T cells producing IL-17A, a proangiogenic cytokine, and decreased density of antitumor Vγ5$^+$ γδ T subsets. Supporting the clinical relevance of our observations, IL-17A$^+$ γδ T cells were detected in human cervical cancer, where HPV oncoproteins are highly expressed, but not in less advanced cervical lesions. These results support the notion that viral oncoproteins can induce a switch from antitumoral to protumoral γδ T subsets in solid tumors.

Author contributions: D.V. and N.J. designed research; D.V.h., B.P., C.H., A.W., V.R., and E.D. performed research; A.W. contributed new reagents/analytic tools; D.V.h., B.P., V.R., L.d.L., P.D., C.J.D., F.B., D.V., and N.J. analyzed data; and D.V. and N.J. wrote the paper.

The authors declare no conflict of interest.

This article is a PNAS Direct Submission. W.K.B. is a guest editor invited by the Editorial Board.

[1]D.V. and N.J. contributed equally to this work.

[2]To whom correspondence may be addressed. Email: dvermijl@ulb.ac.be or n.jacobs@ulg.ac.be.

This article contains supporting information online at www.pnas.org/lookup/suppl/doi:10.1073/pnas.1712883114/-/DCSupplemental.

of Btnl genes by epithelia appears to be a conserved mechanism that shapes local T-cell compartments.

Human papillomavirus (HPV) is a DNA virus that infects keratinocytes of the genital tract mucosa and the skin. Persistent infection with high-risk HPV types may lead to cancers of the anogenital region as well as of the head and neck (21). The world health organization (www.who.int/mediacentre/factsheets/fs380/en/, accessed October 17, 2016) classified uterine cervical cancer as the second most common cancer in women living in less developed regions. This persistent infection with high-risk HPV is associated with the overexpression of the HPV oncoproteins E6 and E7 in nearly all epithelial cells (22, 23). The p53 and retinoblastoma proteins are well-characterized targets of these HPV oncoproteins but more recent studies have shown that the alteration of additional pathways are also important for transformation such as the DNA damage response pathway (24, 25). For example, high-risk HPV E7 has been shown to activate the ATM DNA damage response in keratinocytes (26), a pathway that is implicated in the up-regulation of NKG2D ligands (27).

Besides the well-established protective role of γδ T cells against cancer, more recent studies revealed also tumor-promoting activities, which are often related to the production of IL-17 (28–31). On the other hand, IL-17–producing γδ T cells have been shown to contribute to the anticancer effect of bacillus Calmette–Guerin against bladder carcinoma and to the efficacy of anticancer chemotherapy (32–34). The role of γδ T cells in HPV-induced malignancy is not known. Even in the aforementioned study analyzing the prognostic value of immune cells across 39 tumors, uterine cervical cancer samples were not included (11). Here, we investigated the role of γδ T cells in HPV-induced cancers in a mouse model where the HPV16 early-region genes, including the oncogenes E6 and E7, are specifically expressed in the keratinocytes leading to the formation of malignant SCC (35). We further analyzed a series of biopsies of human HPV-associated squamous intraepithelial lesions (SILs) and SCC. Altogether, our observations support the notion that HPV oncoprotein-induced remodeling of epithelial-associated γδ T-cell populations promotes the cancerous development of HPV-associated lesions.

Results

γδ T Cells Promote the Formation of HPV-Induced Lesions. To address whether γδ T cells play a pro- or antitumor role in HPV-associated lesions, K14-HPV16 mice [a model for HPV-induced carcinogenesis (35), designated here as HPV mice] were crossed with mice lacking γδ T cells (TCRδ$^{-/-}$ mice) (5). The spontaneous formation of lesions on the skin, head, ears, and tail was followed from 6 to 36 wk of age in both HPV and HPV TCRδ$^{-/-}$ mice and scored as described in *SI Appendix*, Fig. S1. Strikingly, the presence of γδ T cells promoted the formation of HPV-induced lesions (Fig. 1). At week 16, around 90% of HPV mice showed a lesion score higher than 7, whereas only 10% of the HPV TCRδ$^{-/-}$ mice reached this score (Fig. 1*B*). Thus, γδ T cells appear to favor the development of HPV oncoprotein-induced skin lesions.

Skint1 Expression and Density of Resident Vγ5$^+$ γδ T Cells (DETCs) Are Reduced in Mice Expressing HPV Oncoproteins in Epidermis. DETCs, the epidermal resident γδ T cells expressing the Vγ5 chain, have been assigned antitumor functions (5, 36). To gain insight into the unexpected protumor role of γδ T cells in the formation of epidermal lesion induced by HPV oncoproteins, we investigated the DETCs in detail in HPV mice before the appearance of severe lesions. At weeks 6–8, the in vivo expression of HPV oncoproteins within keratinocytes is associated with a very significant decrease of Skint1 expression, the skin-specific Btnl member known to be crucial for the presence of DETCs within the skin (17) (Fig. 2*A*). This decrease in Skint1 expression was independent of the presence of γδ T cells (*SI Appendix*, Fig. S2*A*). We also assessed the effect of HPV oncoproteins on the expression of the NKG2D ligand Rae1, as

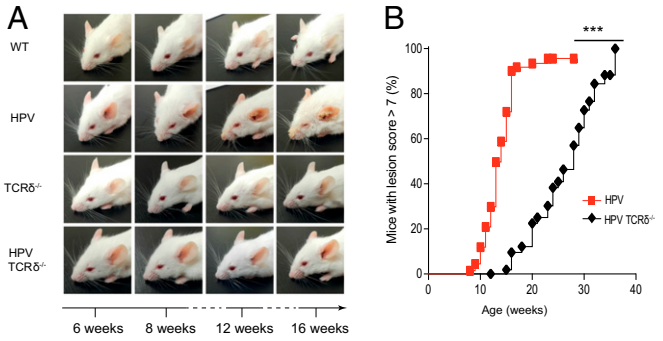

Fig. 1. γδ T cells accelerate the development of HPV-induced lesions in the K14-HPV16 mouse model. (*A*) Ear lesion followup of four males from different genetic backgrounds: WT, HPV, TCR δ$^{-/-}$, and HPV TCR δ$^{-/-}$ at weeks 6, 8, 12, and 16. (*B*) Percentage of HPV and HPVTCRδ$^{-/-}$ mice with a score >7 according to age. HPV ($n = 66$, red line with squares) and HPV TCR δ$^{-/-}$ ($n = 54$, black line with diamonds) mice were observed for 36 wk and assigned a lesion score according to the severity of lesions present on their skin, head, ears, and tail. A score >7 was considered as severe (logrank test, ***$P < 0.001$).

DETCs, especially when activated, express high levels of NKG2D (5, 37). However, unlike Skint1, expression of epidermal Rae1 was not significantly influenced by HPV oncoproteins (*SI Appendix*, Fig. S2*B*). The decrease in Skint1 expression was associated with a clear change in the morphology of the DETCs of HPV mice: they showed a more round shape compared with the classical dendritic cell-like morphology of DETCs in WT mice (Fig. 2 *B* and *C*). Furthermore, quantification of the density of Vγ5$^+$ cells within the epidermis by confocal microcopy revealed a marked reduction in the Vγ5$^+$ cell density in HPV skin (Fig. 2 *B* and *D*). We observed similar results when cell circularity and cell density were quantified for γδTCR^{high} T cells (*SI Appendix*, Fig. S2 *C* and *D*); indeed, high expression of the γδ TCR on skin γδ T cells is known to be derived from Vγ5 expressing γδ T cells (14). Thus, the expression of HPV oncoproteins in keratinocytes causes a decrease of Skint1 expression, which is associated with a reduction in the density of resident antitumor DETCs.

HPV-Oncoprotein Expression in Epidermis Leads to Infiltration of Non-Vγ5 γδ T Cells. Besides the observation via confocal microscopy that the Vγ5$^+$/TCR^{high} cells were reduced in the epidermis of HPV mice, there were indications for the presence of γδTCR^{low} expressing γδ T cells and CD3$^+$γδ$^-$ T cells (Fig. 2*B*, *Inset* arrows). These preliminary observations were investigated further to assess the possible infiltration of other γδ T cells in the epidermis of HPV mice. By using flow cytometry, we showed a reduction in the percentage of Vγ5$^+$/γδTCR^{high} cells in HPV epidermis, which was accompanied by an increase in the percentage of γδTCR^{low} expressing γδ T cells (Fig. 3 *A* and *B*). We observed also an increase in the percentage of CD3$^+$γδ^{neg} T cells in HPV epidermis (Fig. 3*A*) and confirmed that these cells express an αβ TCR (*SI Appendix*, Fig. S3), explaining the decrease in percentage of γδTCR$^+$ cells within CD3$^+$ cells (Fig. 3*B*). Besides the percentage, also the absolute number of γδ TCR^{low} T cells increased significantly in HPV epidermis (*SI Appendix*, Fig. S4*A*). However, the absolute number of Vγ5$^+$/γδTCR^{high} cells did not show a difference. The decrease in density observed by microscopy (Fig. 2*D* and *SI Appendix*, Fig. S2*D*) is thus likely due to the fact that the epidermis of HPV mice is clearly thicker (*SI Appendix*, Fig. S4*B*) than in WT mice. Among the same line, the decrease in percentage of Vγ5$^+$/γδTCR^{high} cells (among γδ T cells) in HPV epidermis can be explained by the huge increase in absolute numbers of γδTCR^{low} cells (*SI Appendix*, Fig. S4*A*). In contrast to the epidermis, no changes in Vγ5$^+$/γδTCR^{high} or γδTCR^{low} percentages (of total γδ T cells) could be observed in

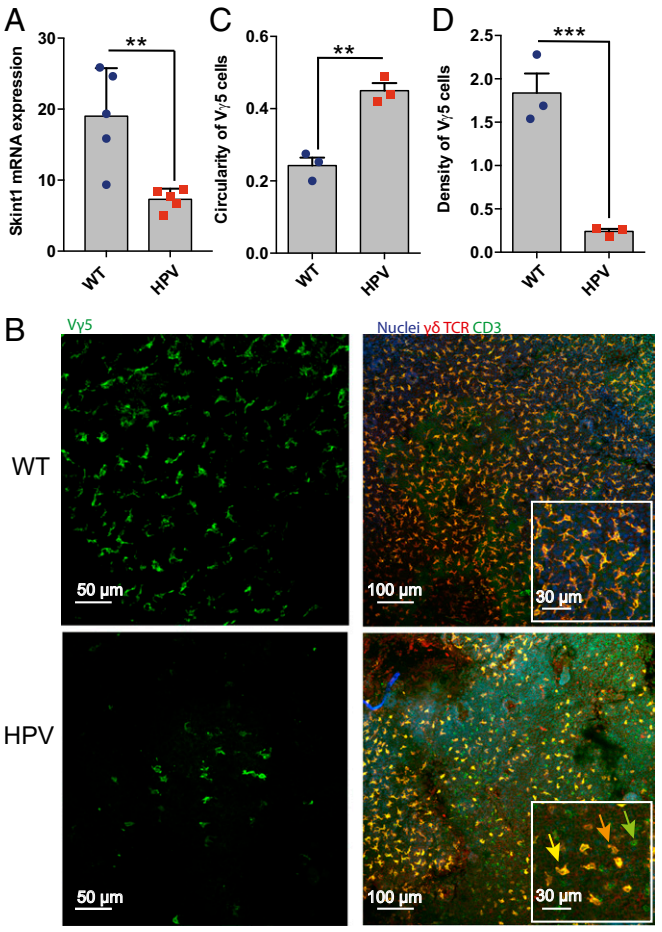

Fig. 2. Reduced Skint1 mRNA expression in HPV mouse epidermis is associated with resident Vγ5 cell (DETCs) morphological and density changes. (*A*) Skint1 mRNA expression was measured by qPCR in WT and HPV mouse epidermis. (*B*) Confocal microscopy pictures of WT and HPV mouse epidermal sheets using anti-Vγ5 antibody (green) (*Left*) or panγδ (red) and anti-CD3 (green) antibodies and DAPI for nuclei staining (blue) (*Right*). Arrows indicate different γδTCR expression intensities: yellow, high intensity; orange, low intensity; green, no γδTCR expression (representative images of three independent experiments). (*C* and *D*) Using ImageJ software, confocal microscopy images of Vγ5 staining in mouse epidermis were used to quantify cell circularity (*C*) and density (*D*) (6- to 7-wk-old mice, Mann–Whitney test, mean + SEM, $^{**}P < 0.01$, $^{***}P < 0.005$).

the dermis (Fig. 3*C*). The lower expression of the γδ TCR within HPV epidermis was not due to activated $Vγ5^+$ DETCs reducing their TCR levels upon activation, as these $γδTCR^{low}$ γδ T cells did not express the Vγ5 chain and are thus not DETCs (Fig. 3*A*). While the Vγ5 chain could still be readily detected by flow cytometry after dispase treatment (*SI Appendix*, Fig. S5*A*) to separate the epidermis from the dermis, this was not the case for Vγ4 (*SI Appendix*, Fig. S5*B*) and Vγ6 (*SI Appendix*, Fig. S5*C*), the main Vγ chains used by dermal γδ T cells (12, 14, 15). Therefore, we used qPCR to obtain further insight into the change in Vγ usage of γδ T cells in the epidermis of HPV mice. The efficiency of the different PCR reactions to quantify the different Vγ chains was similar, allowing comparison of the qPCR data for the different Vγ chains (*SI Appendix*, Fig. S6). We confirmed the decrease in $Vγ5^+$ T-cell density observed by microscopy (Fig. 2*D*) in HPV epidermis at the RNA level (Fig. 3*D*) and decreased Vγ5 RNA showed correlation with lower Skint1 RNA expression (*SI Appendix*, Fig. S2*E*). In parallel, the low level of Vγ5 mRNA expression was accompanied by a significant increase of Vγ6 mRNA (Fig. 3*E*). The Vγ4 chain showed a tendency to be increased in HPV epidermis, but this did not reach statistical difference; the other Vγ chains showed very low expression and were not increased in HPV epidermis (Fig. 3*E*). In sum, HPV-oncoprotein expression within the epidermis leads to the epidermal infiltration of γδ TCR^{low} cells, mainly expressing the Vγ6 chain. We call these cells from now onwards "$γδ^{low}$ T cells."

$γδ^{low}$ T Cells in HPV Epidermis Express High Levels of CCR2 but Reduced Levels of CCR6. As the expression of HPV oncoproteins in the keratinocytes of the epidermis leads to the recruitment of $γδ^{low}$ T cells, we sought to obtain insight into the possible role of chemokine receptors and associated chemokine ligands. Since both CCR2 (imiquimod model of psoriasis) (38) and CCR6 (IL-23 injection model of psoriasis) (39) have been shown to be involved into the recruitment of γδ T cells toward the skin, we focused on these chemokine receptors and associated ligands. Furthermore, CCR6 has been shown to be important for the homeostatic trafficking of γδ T cells, including the Vγ6 subset, to the dermis (15, 40). The $γδ^{low}$ T cells in HPV epidermis showed high expression of CCR2 (Fig. 4*A*). CCR2 expression was also increased on γδ T cells derived from the dermis of HPV mice compared with WT mice (Fig. 4*B*). In sharp contrast, CCR6 expression, which was highly expressed on dermal γδ T cells of WT mice, showed marked reduced expression on HPV dermal γδ T cells and showed only low expression on HPV epidermal $γδ^{low}$ T cells (Fig. 4 *A* and *B*). The high expression of CCR2 on $γδ^{low}$ T cells in the HPV epidermis was associated with an increased expression of the CCR2 ligand CCL2 (the only CCR2 ligand that is not cross-reactive with other chemokine receptors) (41, 42) in the HPV epidermis, while the expression in the HPV dermis was decreased (Fig. 4*C*). Other CCR2 ligands (CCL7 and CCL8), but not all (CCL12), showed differential expression in epidermis and/or dermis of HPV mice (*SI Appendix*, Fig. S7 *A–C*). In contrast, the unique ligand for CCR6, CCL20, did not show differential expression (*SI Appendix*, Fig. S7*D*). Thus, these data indicate that high CCR2 expression, together with reduced expression of CCR6 at the dermal niche, can play an important role in the recruitment of $γδ^{low}$ T cells to the epidermis upon HPV-oncoprotein expression.

$γδ^{low}$ T Cells Produce IL-17A in Epidermis of HPV Oncoprotein-Induced Lesions. Recently, protumor roles of γδ T cells have been linked, at least partially, to their capacity to produce IL-17 (28, 29, 31). Therefore, we assessed whether our observations regarding a protumor role of γδ T cells in HPV-induced lesions and the corresponding reorganization of the epidermal γδ T cell subsets could be linked to the production of IL-17A. Epidermal cell suspensions from HPV mice contained more IL-17A mRNA compared with WT mice (Fig. 5*A*), while no difference was observed for IL-13, an antitumor cytokine recently detected in the epidermal γδ T cells (43) (*SI Appendix*, Fig. S8*A*). By investigating this further at the protein level by flow cytometry, we found that γδ T cells within epidermal cell suspensions derived from HPV mice briefly cultured in vitro, without further stimulation, clearly produced IL-17A, while epidermal γδ T cells from WT mice did not (Fig. 5 *B* and *C*). This spontaneous IL-17A production likely reflects ongoing cell activation in vivo by the HPV keratinocytes. IL-17 production was restricted to $γδT^{low}$ T cells (Fig. 5 *C* and *D*). IL-17 production was further increased upon incubation with the artificial polyclonal stimulation treatment phorbol myristate acetate (PMA) and ionomycin (Fig. 5 *B–D*). We observed also IL-17A production by $CD3^+γδ^-$ cells (Fig. 5*D*), which are presumably Th17 cells. It may be noted that the epidermis of $TCRδ^{-/-}$ HPV mice also displayed increased IL-17A mRNA levels (*SI Appendix*, Fig. S8*B*), possibly due to the reported replacement of "normal" γδ DETCs by "replacement αβ DETCs" (36). However, T cells derived from HPV $TCRδ^{-/-}$ HPV mice did not show HPV-induced spontaneous IL-17 protein expression

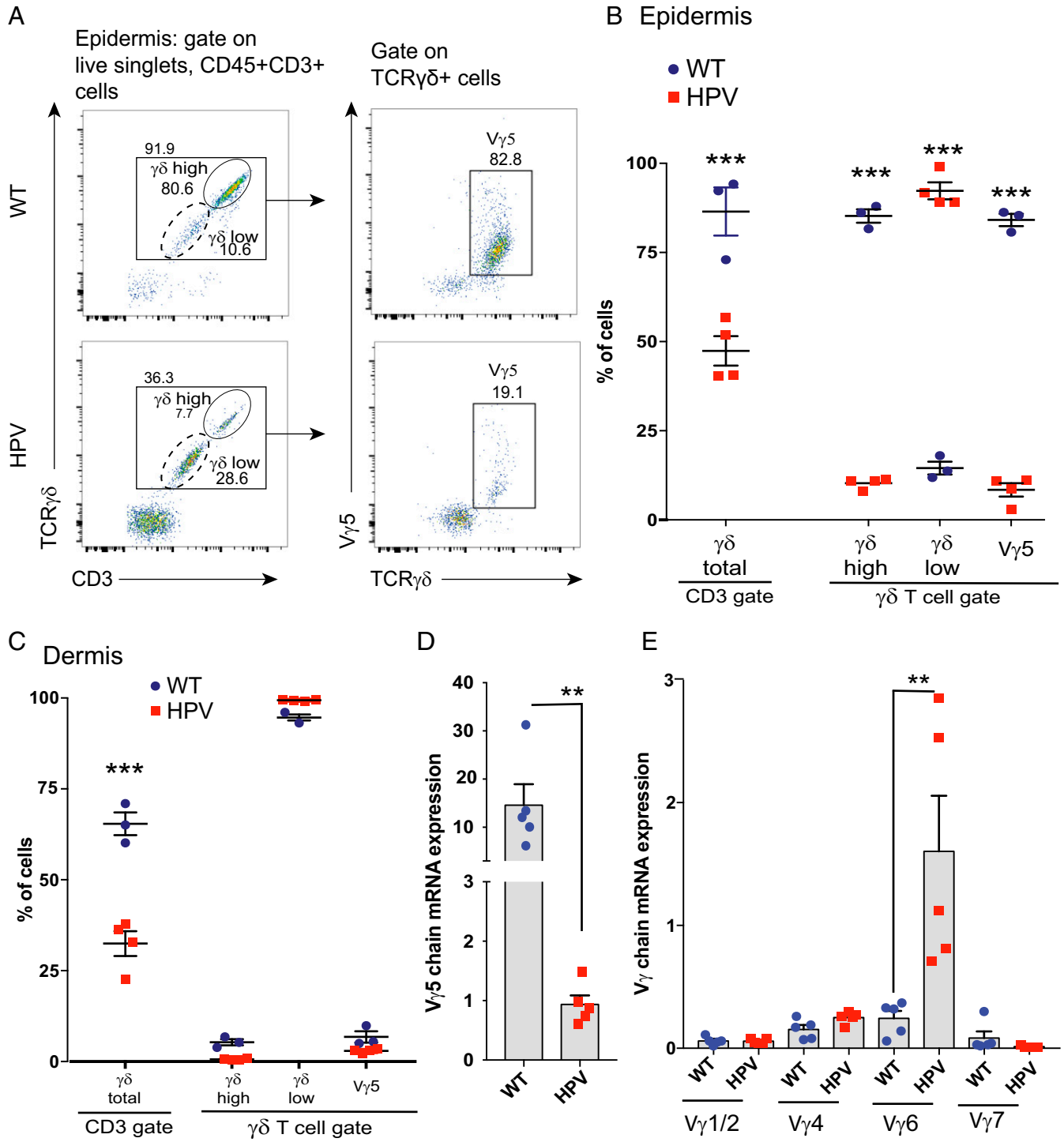

Fig. 3. Decrease of Vγ5^{+} cells in HPV mouse epidermis is associated with an increase of Vγ6^{+} cells. (*A*) FACS dot plots of Vγ5 staining of γδ T cells from epidermal cell suspensions. (*B*–*C*) Percentages of γδ T cells in CD3^{+} T cell gate, γδ TCR^{high}, γδ TCR^{low}, Vγ5^{+} T cells in γδ T cell gate from epidermal (*B*) and dermal (*C*) cell suspensions of WT and HPV. (*D*) Vγ5 (*E*) Vγ1/2, Vγ4, Vγ6, and Vγ7 chain mRNA expression was measured by qPCR in WT and HPV mouse epidermis (6- to 7-wk-old mice, ANOVA test, mean ± SEM, $^{**}P < 0.01$, $^{***}P < 0.005$).

and/or release (*SI Appendix*, Fig. S8*C*), possibly reflecting the need for the correct (γδ) TCR specificities to functionally respond to the HPV oncoprotein-induced changes. Indeed, also the local cancer protection role is provided only by the "real" γδ DETCs and not by replacement αβ DETCs in TCRδ$^{-/-}$ mice (36). Of note, the increase in IL-17–producing T cells in HPV mice was specific for the epidermis, as such an increase was not observed in dermis from the same mice (*SI Appendix*, Fig. S8*D*). Overall, these data indicate that γδ^{low} T cells from the HPV epidermis produce IL-17A in situ upon encountering HPV oncoprotein-transformed keratinocytes.

γδ T Cells Promote HPV Oncoprotein-Induced Angiogenesis in the Skin. Since both HPV oncoproteins and IL-17 have been implicated in angiogenesis (44–46), we investigated blood vessel density by

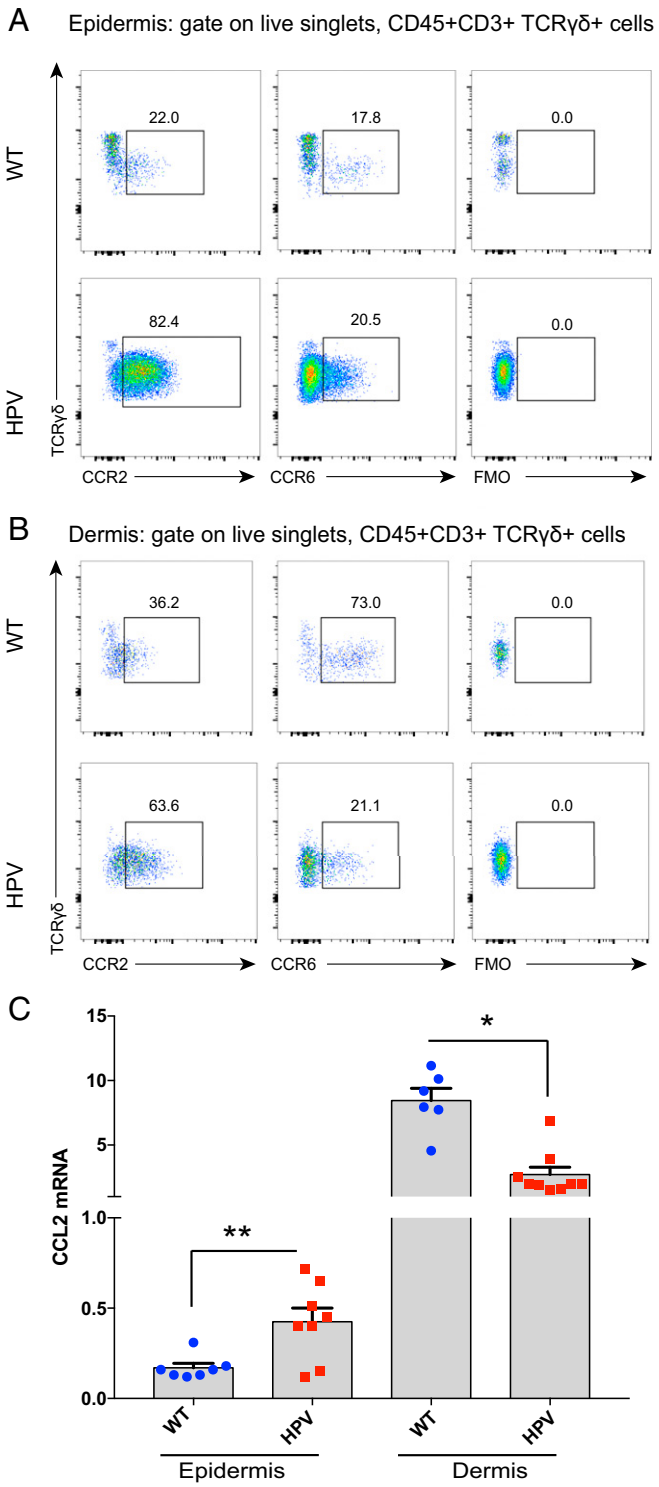

Fig. 4. $\gamma\delta^{low}$ T cells in HPV epidermis express high levels of CCR2 but reduced levels of CCR6. (*A* and *B*) Flow cytometry plots of CCR2 and CCR6 levels on γδ T cells from epidermis (*A*) and dermis (*B*) of WT and HPV mice; representative of three independent experiments. (*C*) qPCR for the CCR2 ligand CCL20 in epidermis and dermis of WT (blue circles) and HPV (red squares) mice (6- to 7-wk-old mice, ANOVA test, means + SEM, $*P < 0.05$, $**P < 0.01$).

immunohistochemistry in ear sections from WT, HPV, $TCR\delta^{-/-}$, and HPV $TCR\delta^{-/-}$ mice. In the presence of γδ T cells, the percentage of blood vessel density was highly increased at weeks 6–8 in epidermis expressing HPV oncoproteins (Fig. 6). However, in HPV $TCR\delta^{-/-}$ mice, this increase was significantly reduced; indeed, dermal blood vessel density reached levels similar to those in mice without expression of the HPV oncoproteins. Thus, this indicates that $\gamma\delta^{low}$ T cells producing locally IL-17A upon encountering HPV-transformed keratinocytes promote the formation of blood vessels in the underlying dermis.

Human Cervical SCC Contains IL-17A–Producing γδ T Cells. To investigate how our results in the murine K14-HPV16 model could translate in human, we verified the presence of γδ T cells and associated IL-17A production in human biopsies of uterine cervix by immunohistochemistry. Biopsies from nonlesional tissue (normal exocervix, Exo), from preneoplastic lesions (SILs) and from cancerous lesions (SCC) were compared. The number of γδ T cells were significantly increased in HPV-associated SCC, but not in SILs, compared with normal exocervix (Fig. 7*A*). This increase in γδ T-cell number was not linked to a general increase of all T cells in these samples (Fig. 7*A*), indicating a preferential γδ T-cell response in SCC samples. On a selected number of samples, a more detailed analysis was performed by dual immunostaining with pan-γδ TCR and IL-17A antibodies. While in some subjects without tumor, $IL\text{-}17A^{+}$ cells could be detected in the epidermis and underlying stroma (Fig. 7*E* and *SI Appendix*, Fig. S9), these $IL\text{-}17A^{+}$ cells were not γδ T cells. However, in SCC biopsies, both in the epidermis and underlying stroma, IL-17A–producing γδ T cells were observed (Fig. 7*C*). Thus, it appears that IL-17A–producing γδ T cells are present in more advanced stages of HPV-induced tumoral lesions (SSC), while γδ T cells detected in normal cervix and in preneoplastic lesions were negative for IL-17A. Overall, the presence of IL-17A–producing γδ T cells in the epidermis upon HPV-oncoprotein overexpression, which leads to cancer development, appears to be a conserved feature in mice and human patients.

Discussion

This study shows that γδ T cells play a protumor role in a mouse model of HPV oncoprotein-induced cancer. Local HPV-oncoprotein expression in the epidermis resulted in a disturbance of the normal γδ T cell subset distribution within the skin and induced the presence of IL-17A–producing $\gamma\delta^{low}$ T-cell subsets in the epidermis, which was associated with increased blood vessel formation in the underlying dermis.

γδ T cells were identified as the most significant favorable prognostic immune population among 39 cancer types (11). However, HPV-induced cancers were not included in this study, despite its high prevalence, especially in developing countries (47) having poor access to the prophylactic vaccine (48). Previous studies that have investigated the role of γδ T cells in epidermis-related tumors have found a clear antitumor role of γδ T cells. In a seminal paper, Girardi et al. (5) showed that mice lacking γδ T cells are highly susceptible to multiple regimens of cutaneous carcinogenesis leading to SCC, either via inoculation of carcinoma cells (intradermal injection with the SCC line PDV) or chemical carcinogenesis [either intradermal injection with the carcinogen methylcholanthrene (MCA) or skin applications of dimethylbenz[a]anthracene (DMBA) and phorbol ester (12-O-tetradecanoylphorbol; TPA), which induce and promote cutaneous malignancy, respectively]. Also inoculation with the widely used B16 melanoma cell line resulted in increased tumor development in γδ T-cell–deficient mice (6). This was followed by other studies using FVB mice (same strain as the HPV16 transgenic mice used in this study) (35), that are highly susceptible to chemically induced SCC (49), where the DMBA + TPA protocol of cutaneous malignancy was used as well. Again, γδ T cells prevented both the chemically induced development of papillomas and their progression into cutaneous SCC, whereas αβ T cells seemed to promote tumor progression (9). Moreover, in the same HPV transgenic oncogene model, $CD4^{+}$ αβ T cells

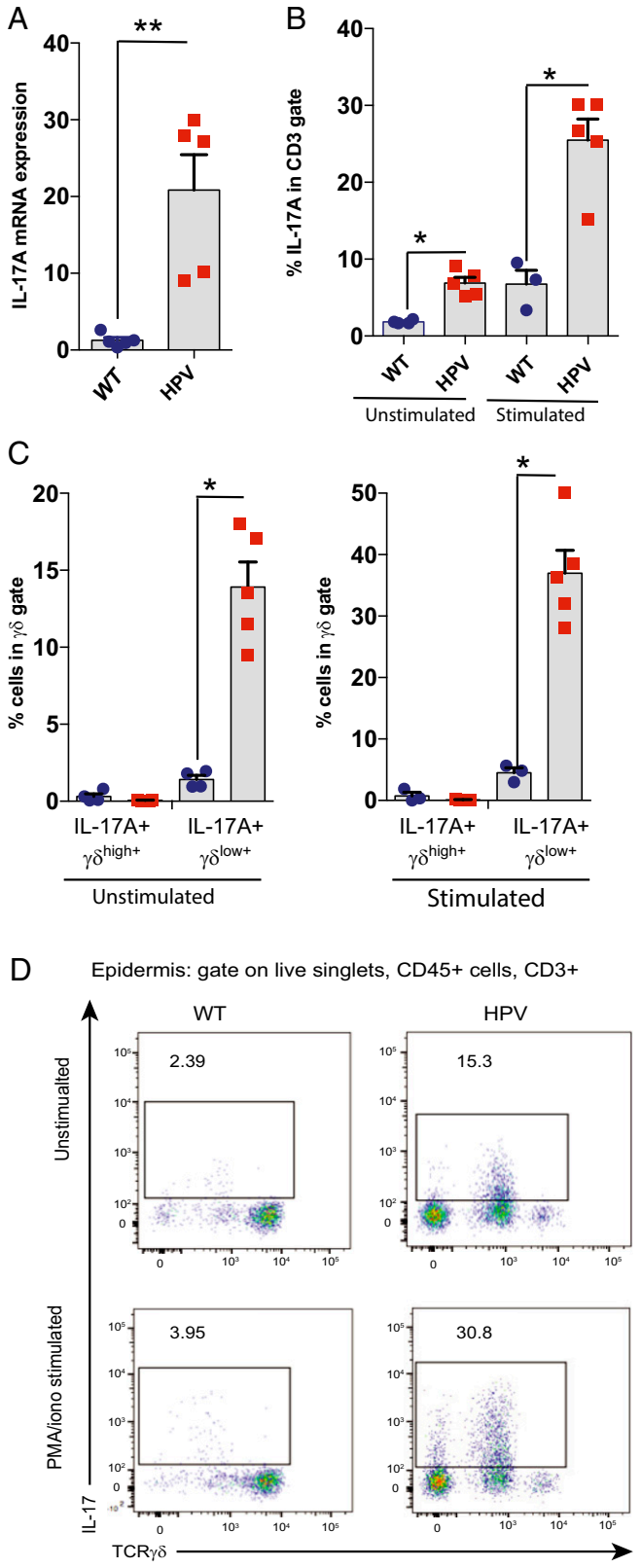

Fig. 5. $\gamma\delta^{low}$ T cells in HPV epidermis produce actively IL-17A. (*A*) IL-17A mRNA expression was measured by qPCR in WT and HPV mouse epidermis. (*B* and *C*) Percentages of IL-17A$^+$ cells determined by FACS intracytoplasmic staining on cells isolated from epidermis and stimulated or not with PMA and ionomycin (*B*, percentages of IL-17A$^+$ cells in CD3$^+$ gate; *C*, percentages of IL-17A$^+$ in TCR $\gamma\delta^+$ gate). (*D*) Representative dot plots of TCR$\gamma\delta^{low+}$ IL-17$^+$ cells in CD3$^+$ gate isolated from epidermis (6- to 7-wk-old mice, Mann–Whitney tests, mean + SEM, $*P < 0.05$, $**P < 0.01$).

have been shown to slightly facilitate tumor development (50). The antitumor role of γδ T cells is (at least partially) attributed to DETCs, emphasizing local immunosurveillance by this resident epidermal γδ T-cell subset (36, 51). In addition, in a mouse model of polyomavirus-induced tumors (polyomavirus is a small DNA tumor virus that carries as well as a potent oncogene with similar mechanisms of action than E6 and E7 from HPV), γδ T cells played a protective role (52). Thus, our finding that γδ T cells clearly promoted HPV oncoprotein-induced lesions was highly unexpected.

The protumor role of γδ T cells that we observed may be related to specific effects mediated by HPV oncoproteins. We found that the local overexpression of these proteins in keratinocytes, the natural host cells for HPV infection, led to a significant reduction of Skint1 expression in the epidermis. Epidermal Skint1 expression is crucial for the presence of DETCs in the skin epidermis and DETC maturation and Skint1 constitutively engages DETCs (19, 20). Thus, HPV oncoprotein-induced down-regulation of Skint1 can provide an explanation for the change in DETC morphology and for their reduction in density within the epidermis. DETCs may play an antitumor role via killing of tumor cells (5) or, as shown more recently in vivo, by tissue regulation of the epithelial barrier via IL-13 (43). The reduction of a particular (protumor) γδ T-cell subset from the epithelial barrier via the decreased expression of the corresponding Btnl member can provide a mechanism to evade the γδ T-cell subset that normally would provide tumor immunosurveillance at the epithelial barrier. In addition, Skint1 has been shown to suppress Sox13, Rorγ, and Bcl11b that are associated with γδ T cells producing IL-17A (19, 20). Thus, reduced Skint1 expression could also allow other γδ T-cell subsets ($\gamma\delta^{low}$ T cells) that produce IL-17A to enter the epidermis. γδ T-cell subsets that normally reside in the dermis, such as the Vγ6$^+$ γδ T-cell subsets, are very motile cells in contrast to immobile DETCs (13–15). In addition, the high CCR2 expression that we observed on γδ T cells in HPV mice and the associated changes in the expression of its ligand CCL2, together with the significant reduction of CCR6 on dermal γδ T cells, can play an important role in this trafficking of γδ T cells from the dermis toward the HPV epidermis upon epidermal HPV-oncoprotein expression. Indeed, it has been recently shown that CCR2 drives recruitment of dermal γδ T cells to inflamed tissues while down-regulation of CCR6 prevents their sequestration into uninflamed dermis (40). Of note, in the B16 melanoma model, the CCR2–CCL2 axis also plays an important role in the recruitment of γδ T cells, but in that model the γδ T cells were not producing IL-17 and had an antitumor role (10). We propose that in the HPV model dermis-derived $\gamma\delta^{low}$ T cells entering the epidermis end up in a "nonnatural" environment and can become activated by HPV-transformed keratinocytes to make IL-17A as revealed by the spontaneous ex vivo IL-17A production from epidermal $\gamma\delta^{low}$ T cells of HPV mice.

HPV-oncoprotein expression resulted in the rounding of DETCs, indicating that they are activated. Rounded DETCs are also observed during wound healing, but DETCs are not reduced in density in this context (53). In contrast, in mice with acute expression of the NKG2D ligand Rae1 in keratinocytes, DETCs become rounded and disappear (36). In epidermis with HPV-oncoprotein expression, however, no up-regulation of Rae1 was observed. Thus, it is more likely that reduction of Skint1, rather than up-regulation of Rae1, contributes to the observed reorganization of the epidermal-associated γδ T cells upon HPV-oncoprotein expression.

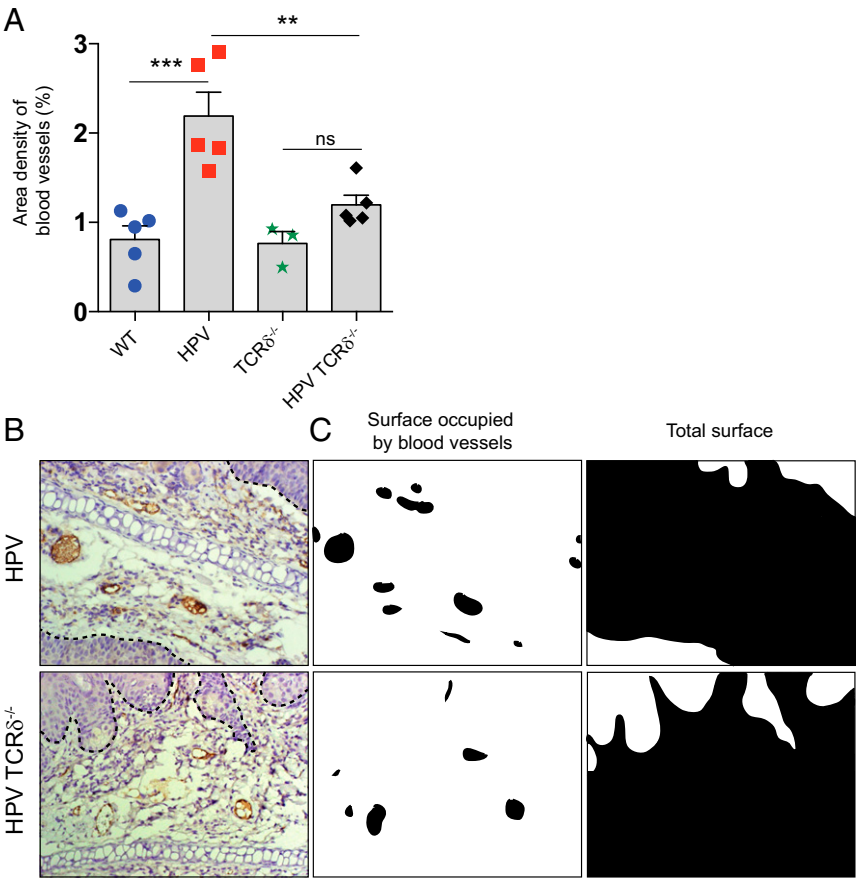

Fig. 6. γδ T cells promote HPV oncoprotein-induced angiogenesis in the skin. (*A*) Blood vessel density, assessed by ImageJ software, in ear sections. Each dot represents the value of one complete ear section. (*B*) Representative images of blood vessels detected with antibodies against VWF in HPV and HPV TCRδ$^{-/-}$ mice. (*C*) ImageJ segmentation of blood vessels and dermis surface. (6- to 7-wk-old mice, ANOVA test, mean + SEM, $^{**}P < 0.01$, $^{***}P < 0.005$; ns, not significant.) (Magnification: *B* and *C*, 10×.)

In a recent study the immunosuppressive role of IL-17A was investigated in a mouse model where the HPV oncoprotein E7 was expressed under a keratin 14 (K14) promoter in a C57BL/6J background (54). Using a skin graft model, the authors demonstrated that IL-17A in HPV16 E7 transgenic skin grafts (E7 being a nonself antigen) inhibited effective host immune responses against the graft but, in contrast to our HPV-transgenic tumor lesion model, no role for γδ T cells could be demonstrated (54). The same study also investigated IL-17 production in CD4$^+$ and γδ T cells from three patients with CIN3 stage of lesion, corresponding to high-grade SILs, and found IL-17 production only in CD4$^+$ T cells, but not in γδ T cells (54). However, they did not investigate SCC samples. Only at that stage, we could clearly identify the presence of IL-17 producing γδ T cells, while these cells were absent in SILs.

Angiogenesis, the process of forming new blood vessels from preexisting ones, has been identified as a crucial factor for cervical cancer growth (55, 56). Of note, it has been shown that the HPV16 oncoproteins E6 and E7, via degradation of p53 and inactivation of retinoblastoma protein (pRB), respectively, result in the up-regulation of vascular endothelial growth factor (VEGF) in keratinocytes, promoting angiogenesis and tumor growth (44, 45). Moreover, E6 appears to promote VEGF in a p53 independent way (44). Also IL-17 can induce the expression of proangiogenic factors, including VEGF, from stromal or tumor cells and it can enhance VEGF-induced vascular endothelial cell growth (46, 57). We have shown here that γδ T cells are necessary for increased angiogenesis in the dermis of HPV16-E6/E7 oncogene transgenic mice. This may be due to the dermal-derived γδ^{low} T cells producing IL-17A in the epidermis upon recognition of E6/E7-transformed keratinocytes. This local IL-17A production may on one hand further increase the expression of the E6/E7-induced VEGF, and on the other hand, act synergistically with VEGF in the promotion of the growth of vascular endothelial cells.

Several treatments are currently approved for HPV-associated diseases. Imiquimod is used to treat early stage lesions such as genital warts or vulvar preneoplasic lesions, but not uterine cervical cancer (58). On the other hand, bevacizumab, a recombinant humanized monoclonal anti-VEGF antibody, was recently approved for the treatment of patients with metastatic, recurrent, or persistent cervical SCCs (56). Our finding that IL-17A–producing γδ T cells can be specifically found within biopsies of HPV-induced SCCs, together with our data generated in the mouse HPV16-transgenic model as described above, points toward a possible contribution of these cells to the increased angiogenesis during SCC cancer development. Targeting IL-17A (e.g., with the anti–IL-17A mAb secukinumab) and/or γδ T cells in this setting may enhance the therapeutic efficacy of bevacizumab. Imiquimod is an agonist Toll-like receptor 7, which induces up-regulation of type I IFN and activation of dendritic cells (59), and treatment of mouse skin with imiquimod is used as a murine model for psoriasis. This drug treatment induces the recruitment of γδ T-producing IL-17A (38, 60). Moreover, in human psoriatic lesions γδ T cells secreting IL-17A have been observed (60, 61). Since our data indicate a protumor role of IL-17–producing γδ T cells in HPV oncoprotein-induced cancer, new clinical trials (62) using imiquimod in HPV-induced pathology context should take into account this population of IL-17A$^+$ γδ T cells.

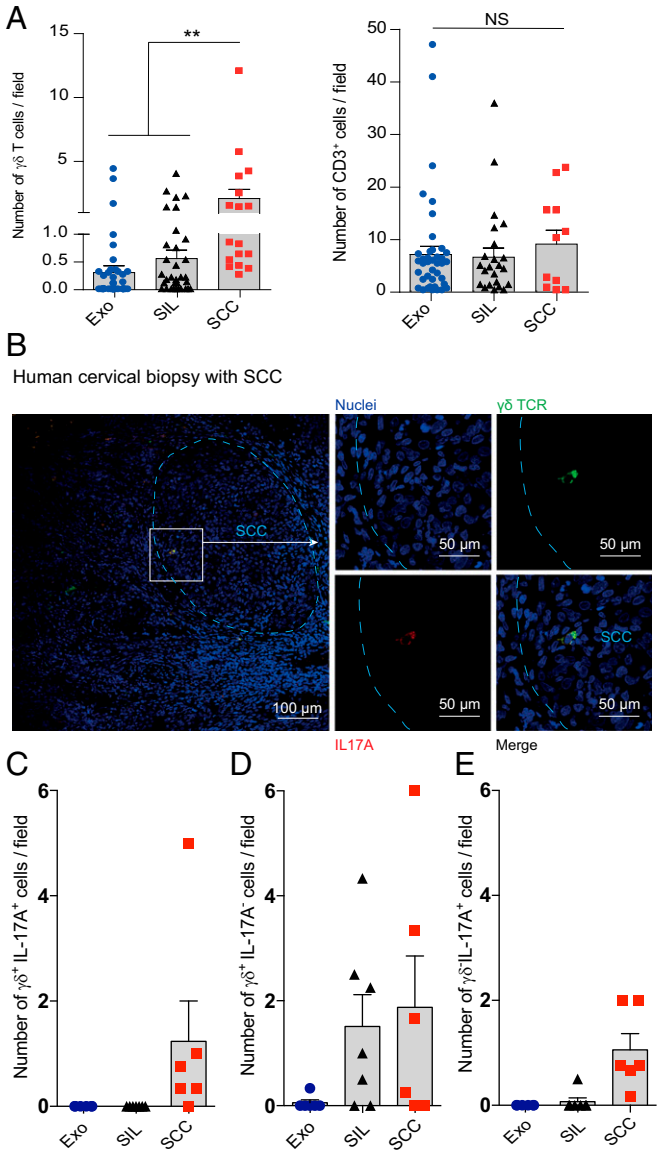

Fig. 7. Human cervical squamous cell carcinoma (SCC) contains IL-17A-producing γδ T cells. (*A*) Quantification of human γδ and total ($CD3^+$) T cells in epidermis of paraffin sections from nonlesional (Exo), preneoplasic lesions (SILs), and tumoral (SCC) biopsies. (*B*) Representative image of a γδ T cell producing IL-17A in SCC (dotted line shows the tumor border). (*C*–*E*) Quantification of human $γδ^+$ $IL\text{-}17A^+$ (*C*), $γδ^+$ $IL\text{-}17^-$ (*D*), and $γδ^-$ $IL\text{-}17A^+$ (*E*) T cells in epidermis of paraffin sections from nonlesional (Exo), preneoplasic lesions (SILs), and tumoral (SCC) biopsies (Kruskal–Wallis test, followed by Dunn's tests for multiple comparisons, mean + SEM, $^{**}P < 0.01$; NS, not significant).

Materials and Methods

Animals. All mouse experiments were conducted in accordance with the guidelines of the local ethical committee of the University of Liège (Belgium). FVBn mice (designated as WT mice) were bred in-house. K14-HPV16 transgenic FVB/n mice (designated as HPV mice) (35) were obtained from Jeffrey Arbeit, Washington University, St. Louis, through the National Cancer Institute Mouse Repository. $TCRδ^{-/-}$ mice in FVB/n background (5) were generously donated by M. Girardi, Yale University, New Haven, CT, and bred in-house. To generate K14-HPV16 mice deficient in γδ T cells, hemizygous K14-HPV16 mice were crossed with $TCRδ^{-/-}$ mice and the K14-HPV16–expressing progeny backcrossed with homozygous $TCRδ^{-/-}$ mice. All mice were used at 6–36 wk of age and were age matched for all experiments. To compare HPV-induced lesions development between K14-HPV16 and K14-HPV16 $TCRδ^{-/-}$ mice a lesion scoring system was established (*SI Appendix*, Fig. S1). A total score was assigned to mice corresponding to the sum of ear, skin, head, and tail/anus lesion appearance. A total score >7 was considered as severe.

RNA Extraction and Real-Time Quantitative PCR. Epidermis RNA was extracted with Direct-Zol (Zymo Research) according to the manufacturer's protocol. We confirmed the quantity of RNA with a NanoDrop. cDNA was synthesizes with a RevertAid H Minus First-Strand cDNA Synthesis Kit (Thermo Scientific). SYBR Green PCR was performed in duplicate to determine mRNA levels in Vγ chains, Skint1, Rae1, and IL-17 and the mRNA levels were normalized to reference genes (ubiquitin C, UBC, and TATA-box binding protein, TBP). Primers are listed in (*SI Appendix*, Table S1).

Immunofluorescent Staining and Morphological Analysis. Epidermal sheets were obtained from the ear skin as previously described (36, 53). Briefly, after hair removal, dorsal and ventral halves were incubated in 0.5 M of ammonium thiocyanate for 20 min at 37 °C. Epidermal sheets were separated from the dermis, fixed in acetone, and stained with antibodies to detect $CD3^+$, $γδ^+$, and $Vγ5^+$ cells (antibodies are listed in *SI Appendix*, Table S2). DAPI (Thermo Fisher) was used to visualize nuclei. The stained sheets were rinsed in PBS and mounted on slides with Eukitt medium (Fluka Analytical). Images were acquired with a confocal microscope (Leica SP5) and transformed into binary pictures using ImageJ. γδ T-cell density and circularity were calculated using ImageJ sofware.

Human uterine cervical biopsies presenting normal exocervix, squamous intraepithelial lesions, or squamous cell carcinoma were stained with anti-pan γδ and anti–IL-17A antibodies (*SI Appendix*, Table S3). Alexa Fluor 488 and 594 coupled with streptavidin were used to visualize positive cells with a Leica SP5 confocal microscope. DAPI staining was used to visualize nuclei and single and double positive cells were counted in the normal or lesional epidermis and in the underlying stroma. For normal exocervix samples, the counting fields (40× magnification) were limited to the epithelium and to the corresponding underlying conjunctive tissue. Concerning samples with lesions (precancerous and cancerous, previously characterized by an anatomopathologist), the counting fields (40× magnification) were limited to the epithelium displaying cervical lesion (precancerous or cancerous, respectively) and to the corresponding underlying conjunctive tissue. Number of counting fields varied between samples from four to eight.

Epidermal and Dermal Cell Suspensions for Flow Cytometry Analyses. Epidermal and dermal cells were prepared from the ear skin. After physical separation, dorsal and ventral halves were incubated in 2.5 units/mL of dispase II (Roche) for 1 h at 37 °C. Epidermal and dermal sheets were separated, cut into small pieces using scissors, and further digested separately using collagenase type IV (1 mg/mL; Sigma) for 1 h at 37 °C. The resulting suspensions were mechanically disrupted using 18-G needles and syringes. Cells were collected through 70-μm cell strainer to be further analyzed by flow cytometry (FACScanto II). To test the reactivity and sensitivity to dispase treatment of different Vγ chain antibodies, we used whole skin prepared as above but without first the separation of epidermal and dermal sheets. This whole skin cell suspension was then treated or not with dispase. In addition to whole skin suspension, we used cell suspension derived from the uterus, known to be highly enriched for γδ T cells expressing the Vγ6 chain (12).

Before surface staining, cells were Fc blocked with anti-CD16/32 (*SI Appendix*, Table S2) for 10 min at 4 °C. Cells were stained 30 min at 4 °C with antibodies (*SI Appendix*, Table S2). To exclude dead cells from the analysis, we added Viability Dye eFluor 780 (eBioscience) before surface staining. For $Vγ6^+$ staining, we used a protocol that combines the GL3 (anti-TCRγδ) and 17D1 (anti-Vγ5/Vγ6) monoclonal antibodies (63). For intracellular cytokine staining, cells were incubated 4 h at 37 °C in the presence of brefeldin A (10 μg/mL; eBioscience) and with or without PMA (6.25 ng/mL; Sigma) and ionomycine (3.3 μg/mL; Sigma). Perm/Fix (BD Biosciences) was used according to the manufacturer instructions and cells were stained for IL-17A. Cells were analyzed on a FACS Canto II (BD Biosciences). Data analysis was performed using FlowJo, LLC with the gating strategy described in *SI Appendix*, Fig. S10. Absolute cell numbers were obtained from total numbers of epidermal and dermal cells.

Immunohistochemistry. Mouse ear tissue sections of 5 mm were deparaffinized and rehydrated through graded xylene and alcohol series. The slides were heated in target retrieval or EDTA buffers (Zytomed Systems) for antigen retrieval in a pressure cooker for 11 min and incubated with anti-Von Willebrand Factor (VWF) antibody (*SI Appendix*, Table S2) for 1 h at room temperature after blocking nonspecific binding with protein block serum free (Dako) for 10 min. Sections were then incubated with TSA system (Perkin-Elmer) or with peroxidase-labeled polymer conjugated to goat anti-rabbit

immunglobulins (Dako EnVision). Antibodies were visualized using diaminobenzidine (Dako). Pictures of complete ear sections stained with anti-VWF were used to calculate the percentage of dermis occupied by blood vessels as described in ref. 64. Briefly, after manual blind segmentation by two independent observers, the blood vessel density of complete ear sections was calculated with ImageJ software.

Human cervical tissues (45 normal exocervix, 33 SIL samples, and 17 SCC samples) were provided, in agreement with the local ethical committee (ethical national number B707201112047), by the GIGA Biothèque, which performed informed consent procedures. For pan-γδ staining, slides were heated in a water bath for 45 min at 99 °C and treated with the CSA II kit (Dako) and stained with mouse anti-human TCRγ constant chain antibody (*SI Appendix*, Table S3). For CD3 staining, slides were heated in EDTA buffer for antigen retrieval in a pressure cooker for 11 min. Sections were incubated with polyclonal rabbit anti-human CD3 (*SI Appendix*, Table S3) for 1 h. Universal LSAB II kit/HRP (Dako) was used to detect primary antibody. Pan-γδ and CD3 staining were visualized using diaminobenzidine (Dako).

Statistical Analysis. Statistical analyses were performed using R (version 3.2.4) and Prism (GraphPad Software) (65). Raw data were transformed where needed and back transformed for graphical presentation. Respect of the assumptions of normal distribution of residuals and homoscedasticity in linear models was verified using diagnostic plots.

ACKNOWLEDGMENTS. We thank Robert Tigelaar (Yale University) and Immo Prinz (Hannover Medical School) for the kind donation of 17D1 antibody; Witold Kedzia and Dominik Pruski (Poznan University of Medical Sciences) for human biopsy samples; Michael Girardi (Yale University) for TCRδ$^{-/-}$ mice; Jeffrey Arbeit (Washington University) for HPV mice; Olga Sobolev (from Adrian Hayday's laboratory, King's College London) for epithelial sheet protocols; Dimitri Pirotin for help in PCR primer design; and the Biothèque, the Immunohistochemistry, and the Flow Cytometry Facilities of the University of Liège. The study was financed through grants from the Fonds National de la Recherche Scientifique (F.R.S.-FNRS; to N.J. and D.V.), the Centre Anticancéreux près l'Université de Liège (to N.J.), the Fonds Léon Fredericq (University of Liège) (to D.V.h. and N.J.), and the Fonds Van Buuren (Université Libre de Bruxelles) (to D.V.).

1. Chien Y-H, Meyer C, Bonneville M (2014) γδ T cells: First line of defense and beyond. *Annu Rev Immunol* 32:121–155.
2. Vantourout P, Hayday A (2013) Six-of-the-best: Unique contributions of γδ T cells to immunology. *Nat Rev Immunol* 13:88–100.
3. Silva-Santos B, Serre K, Norell H (2015) γδ T cells in cancer. *Nat Rev Immunol* 15:683–691.
4. Itohara S, et al. (1993) T cell receptor delta gene mutant mice: Independent generation of alpha beta T cells and programmed rearrangements of gamma delta TCR genes. *Cell* 72:337–348.
5. Girardi M, et al. (2001) Regulation of cutaneous malignancy by gammadelta T cells. *Science* 294:605–609.
6. Gao Y, et al. (2003) Gamma delta T cells provide an early source of interferon gamma in tumor immunity. *J Exp Med* 198:433–442.
7. Liu Z, et al. (2008) Protective immunosurveillance and therapeutic antitumor activity of gammadelta T cells demonstrated in a mouse model of prostate cancer. *J Immunol* 180:6044–6053.
8. Street SEA, et al. (2004) Innate immune surveillance of spontaneous B cell lymphomas by natural killer cells and gammadelta T cells. *J Exp Med* 199:879–884.
9. Girardi M, et al. (2003) The distinct contributions of murine T cell receptor (TCR)gammadelta+ and TCRalphabeta+ T cells to different stages of chemically induced skin cancer. *J Exp Med* 198:747–755.
10. Lança T, et al. (2013) Protective role of the inflammatory CCR2/CCL2 chemokine pathway through recruitment of type 1 cytotoxic γδ T lymphocytes to tumor beds. *J Immunol* 190: 6673–6680.
11. Gentles AJ, et al. (2015) The prognostic landscape of genes and infiltrating immune cells across human cancers. *Nat Med* 21:938–945.
12. Vermijlen D, Prinz I (2014) Ontogeny of innate T lymphocytes:–Some innate lymphocytes are more innate than others. *Front Immunol* 5:486, and erratum (2015) 6: 624.
13. Gray EE, Suzuki K, Cyster JG (2011) Cutting edge: Identification of a motile IL-17-producing gammadelta T cell population in the dermis. *J Immunol* 186:6091–6095.
14. Sumaria N, et al. (2011) Cutaneous immunosurveillance by self-renewing dermal gammadelta T cells. *J Exp Med* 208:505–518.
15. Cai Y, et al. (2014) Differential developmental requirement and peripheral regulation for dermal Vγ4 and Vγ6T17 cells in health and inflammation. *Nat Commun* 5:3986.
16. Chodaczek G, Papanna V, Zal MA, Zal T (2012) Body-barrier surveillance by epidermal γδ TCRs. *Nat Immunol* 13:272–282.
17. Barbee SD, et al. (2011) Skint-1 is a highly specific, unique selecting component for epidermal T cells. *Proc Natl Acad Sci USA* 108:3330–3335.
18. Boyden LM, et al. (2008) Skint1, the prototype of a newly identified immunoglobulin superfamily gene cluster, positively selects epidermal gammadelta T cells. *Nat Genet* 40:656–662.
19. Turchinovich G, Hayday AC (2011) Skint-1 identifies a common molecular mechanism for the development of interferon-γ-secreting versus interleukin-17-secreting γδ T cells. *Immunity* 35:59–68.
20. Di Marco Barros R, et al. (2016) Epithelia use butyrophilin-like molecules to shape organ-specific γδ T cell compartments. *Cell* 167:203–218.e17.
21. zur Hausen H (2002) Papillomaviruses and cancer: From basic studies to clinical application. *Nat Rev Cancer* 2:342–350.
22. Dürst M, Glitz D, Schneider A, zur Hausen H (1992) Human papillomavirus type 16 (HPV 16) gene expression and DNA replication in cervical neoplasia: Analysis by in situ hybridization. *Virology* 189:132–140.
23. Ressler S, et al. (2007) High-risk human papillomavirus E7 oncoprotein detection in cervical squamous cell carcinoma. *Clin Cancer Res* 13:7067–7072.
24. Moody CA, Laimins LA (2010) Human papillomavirus oncoproteins: Pathways to transformation. *Nat Rev Cancer* 10:550–560.
25. Langsfeld ES, Bodily JM, Laimins LA (2015) The deacetylase sirtuin 1 regulates human papillomavirus replication by modulating histone acetylation and recruitment of DNA damage factors NBS1 and Rad51 to viral genomes. *PLoS Pathog* 11:e1005181.
26. Moody CA, Laimins LA (2009) Human papillomaviruses activate the ATM DNA damage pathway for viral genome amplification upon differentiation. *PLoS Pathog* 5: e1000605–e1000613.
27. Gasser S, Orsulic S, Brown EJ, Raulet DH (2005) The DNA damage pathway regulates innate immune system ligands of the NKG2D receptor. *Nature* 436:1186–1190.
28. Wakita D, et al. (2010) Tumor-infiltrating IL-17-producing gammadelta T cells support the progression of tumor by promoting angiogenesis. *Eur J Immunol* 40:1927–1937.
29. Rei M, et al. (2014) Murine CD27(–) Vγ6(+) γδ T cells producing IL-17A promote ovarian cancer growth via mobilization of protumor small peritoneal macrophages. *Proc Natl Acad Sci USA* 111:E3562–E3570.
30. Coffelt SB, et al. (2015) IL-17-producing γδ T cells and neutrophils conspire to promote breast cancer metastasis. *Nature* 522:345–348.
31. Patil RS, et al. (2016) IL17 producing γδT cells induce angiogenesis and are associated with poor survival in gallbladder cancer patients. *Int J Cancer* 139:869–881.
32. Takeuchi A, et al. (2011) IL-17 production by γδ T cells is important for the antitumor effect of Mycobacterium bovis bacillus Calmette-Guérin treatment against bladder cancer. *Eur J Immunol* 41:246–251.
33. Ma Y, et al. (2011) Contribution of IL-17-producing gamma delta T cells to the efficacy of anticancer chemotherapy. *J Exp Med* 208:491–503.
34. Mattarollo SR, et al. (2011) Pivotal role of innate and adaptive immunity in anthracycline chemotherapy of established tumors. *Cancer Res* 71:4809–4820.
35. Coussens LM, Hanahan D, Arbeit JM (1996) Genetic predisposition and parameters of malignant progression in K14-HPV16 transgenic mice. *Am J Pathol* 149:1899–1917.
36. Strid J, et al. (2008) Acute upregulation of an NKG2D ligand promotes rapid reorganization of a local immune compartment with pleiotropic effects on carcinogenesis. *Nat Immunol* 9:146–154.
37. Nitahara A, et al. (2006) NKG2D ligation without T cell receptor engagement triggers both cytotoxicity and cytokine production in dendritic epidermal T cells. *J Invest Dermatol* 126:1052–1058.
38. Ramírez-Valle F, Gray EE, Cyster JG (2015) Inflammation induces dermal Vγ4+ γδT17 memory-like cells that travel to distant skin and accelerate secondary IL-17-driven responses. *Proc Natl Acad Sci USA* 112:8046–8051.
39. Mabuchi T, et al. (2013) CCR6 is required for epidermal trafficking of γδ-T cells in an IL-23-induced model of psoriasiform dermatitis. *J Invest Dermatol* 133:164–171.
40. McKenzie DR, et al. (2017) IL-17-producing γδ T cells switch migratory patterns between resting and activated states. *Nat Commun* 8:15632.
41. Zlotnik A, Yoshie O (2012) The chemokine superfamily revisited. *Immunity* 36: 705–716.
42. Griffith JW, Sokol CL, Luster AD (2014) Chemokines and chemokine receptors: Positioning cells for host defense and immunity. *Annu Rev Immunol* 32:659–702.
43. Dalessandri T, Crawford G, Hayes M, Castro Seoane R, Strid J (2016) IL-13 from intraepithelial lymphocytes regulates tissue homeostasis and protects against carcinogenesis in the skin. *Nat Commun* 7:12080.
44. López-Ocejo O, et al. (2000) Oncogenes and tumor angiogenesis: The HPV-16 E6 oncoprotein activates the vascular endothelial growth factor (VEGF) gene promoter in a p53 independent manner. *Oncogene* 19:4611–4620.
45. Toussaint-Smith E, Donner DB, Roman A (2004) Expression of human papillomavirus type 16 E6 and E7 oncoproteins in primary foreskin keratinocytes is sufficient to alter the expression of angiogenic factors. *Oncogene* 23:2988–2995.
46. Numasaki M, et al. (2003) Interleukin-17 promotes angiogenesis and tumor growth. *Blood* 101:2620–2627.
47. Ferlay J, et al. (2010) Estimates of worldwide burden of cancer in 2008: GLOBOCAN 2008. *Int J Cancer* 127:2893–2917.
48. Campos NG, Sharma M, Clark A, Kim JJ, Resch SC (2016) Resources required for cervical cancer prevention in low- and middle-income countries. *PLoS One* 11: e0164000–e0164020.
49. Hennings H, et al. (1993) FVB/N mice: An inbred strain sensitive to the chemical induction of squamous cell carcinomas in the skin. *Carcinogenesis* 14:2353–2358.
50. Daniel D, et al. (2003) Immune enhancement of skin carcinogenesis by CD4+ T cells. *J Exp Med* 197:1017–1028.
51. Hayday AC (2009) Gammadelta T cells and the lymphoid stress-surveillance response. *Immunity* 31:184–196.
52. Mishra R, Chen AT, Welsh RM, Szomolanyi-Tsuda E (2010) NK cells and gammadelta T cells mediate resistance to polyomavirus-induced tumors. *PLoS Pathog* 6:e1000924.
53. Jameson J, et al. (2002) A role for skin gammadelta T cells in wound repair. *Science* 296:747–749.

54. Gosmann C, Mattarollo SR, Bridge JA, Frazer IH, Blumenthal A (2014) IL-17 suppresses immune effector functions in human papillomavirus-associated epithelial hyperplasia. *J Immunol* 193:2248–2257.
55. Stafl A, Mattingly RF (1975) Angiogenesis of cervical neoplasia. *Am J Obstet Gynecol* 121:845–852.
56. Bizzarri N, et al. (2016) Bevacizumab for the treatment of cervical cancer. *Expert Opin Biol Ther* 16:407–419.
57. Takahashi H, Numasaki M, Lotze MT, Sasaki H (2005) Interleukin-17 enhances bFGF-, HGF- and VEGF-induced growth of vascular endothelial cells. *Immunol Lett* 98: 189–193.
58. de Witte CJ, et al. (2015) Imiquimod in cervical, vaginal and vulvar intraepithelial neoplasia: A review. *Gynecol Oncol* 139:377–384.
59. Stary G, et al. (2007) Tumoricidal activity of TLR7/8-activated inflammatory dendritic cells. *J Exp Med* 204:1441–1451.
60. Cai Y, et al. (2011) Pivotal role of dermal IL-17-producing γδ T cells in skin inflammation. *Immunity* 35:596–610.
61. Laggner U, et al. (2011) Identification of a novel proinflammatory human skin-homing Vγ9Vδ2 T cell subset with a potential role in psoriasis. *J Immunol* 187:2783–2793.
62. Koeneman MM, et al. (2016) TOPical imiquimod treatment of high-grade cervical intraepithelial neoplasia (TOPIC trial): Study protocol for a randomized controlled trial. *BMC Cancer* 16:132.
63. Roark CL, et al. (2004) Subset-specific, uniform activation among V gamma 6/V delta 1+ gamma delta T cells elicited by inflammation. *J Leukoc Biol* 75:68–75.
64. Masset A, et al. (2011) Unimpeded skin carcinogenesis in K14-HPV16 transgenic mice deficient for plasminogen activator inhibitor. *Int J Cancer* 128:283–293.
65. R Development Core Team (2016) R: A Language and Environment for Statistical Computing (R Foundation for Statistical Computing, Vienna). Available at https://www.R-project.org/. Accessed September 1, 2016.

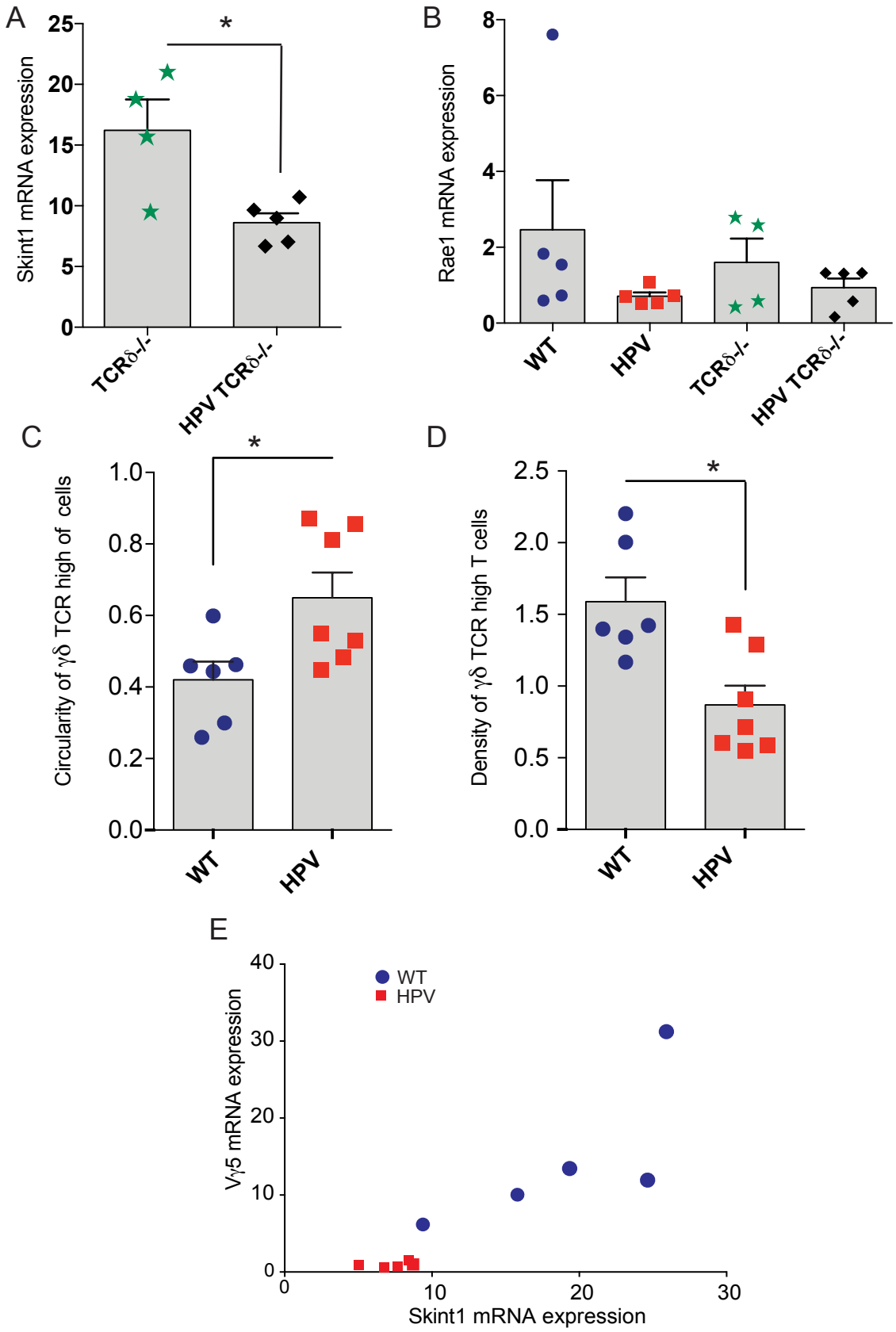

Fig. S2. Expression of Skint1 and Rae1 in epidermal sheets and morphological and density changes of T cells expressing high level of γδTCR.

(A) Skint1 mRNA expression was measured by qPCR in TCRδ-/- and HPV TCRδ-/- mouse epidermis (t-test, mean + SEM, * p<0.05). (B) Rae1 mRNA expression was measured by qPCR in WT, HPV, TCR δ-/- and HPV TCRδ-/- mouse epidermis (mean + SEM). (C-D) Using ImageJ software, confocal microscopy images of pan γδ TCR and anti-CD3 staining in mouse epidermis were used to quantify cell circularity (C) and density (D) (Mann-Whitney test, mean + SEM, * = p < 0.05). (E) Correlation between Skint1 and Vγ5. Correlation between mRNA expression of Skint1 and Vγ5 chains measured by qPCR in WT (blue circles) and HPV (red squares) mouse epidermis. Each dot represents the Skint1 and Vγ5 mRNA expression data derived from the same epidermal RNA sample (ancova test, p= 0.0146).

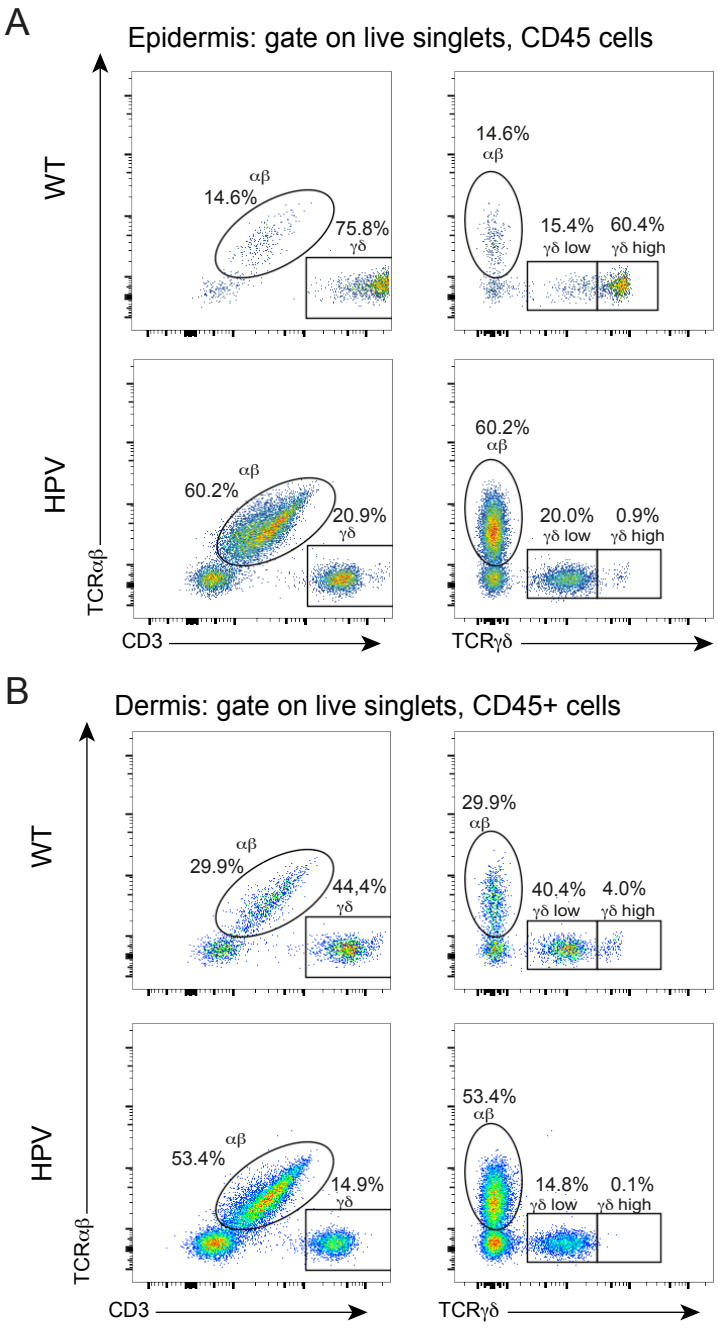

Fig. S3. CD3, γδ and αβ TCR flow cytometry staining in epidermis (A) and dermis (B) of WT and HPV mice.

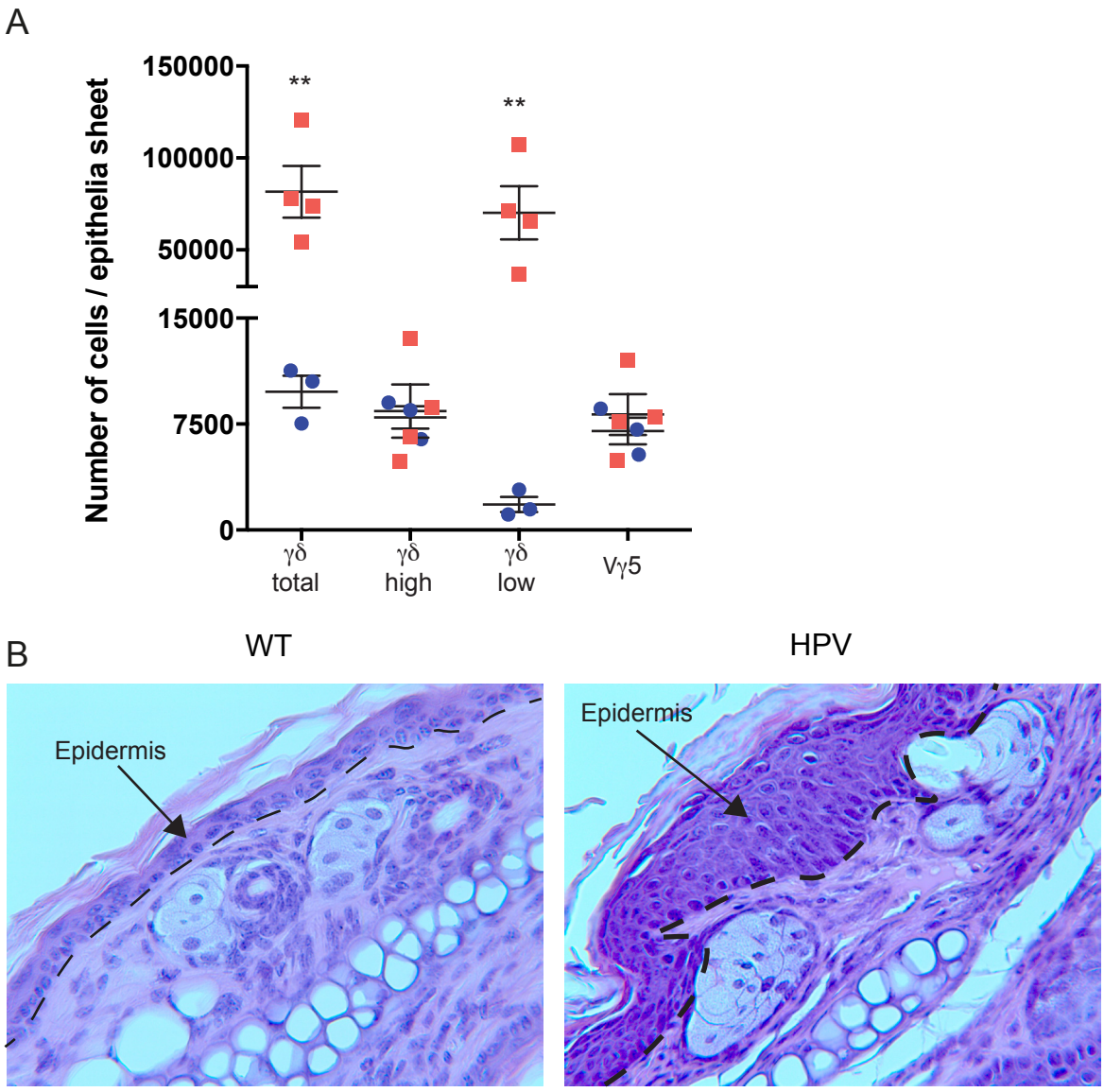

Fig. S4. (A) Absolute numbers of γδ T cells, γδ T TCRhigh, γδ T TCRlow, Vγ5+ from epidermal cell suspension (anova test, mean ± SEM, ** = $p < 0.01$). (B) Ear section histology showing the thickness (above the dotted line) of WT and HPV epidermis (representative images of week-7 mice from at least 3 independent experiences).

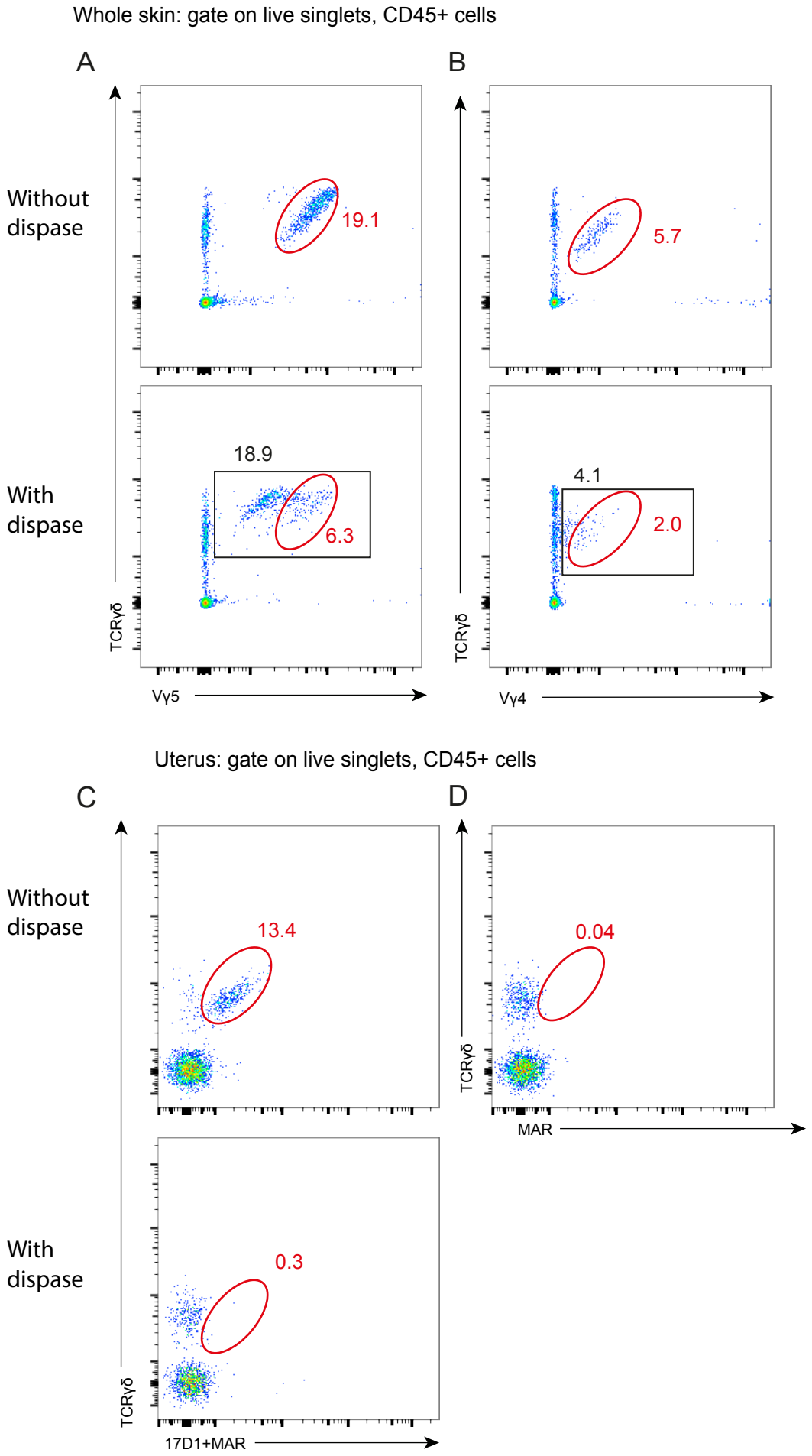

Fig. S5: Impact of dispase treatment on Vγ5 (A), Vγ4(B) and Vγ6 (C) staining.
(A-B) Facs dot plots of Vγ5 (A), Vγ4 (B), of CD45+ live cells from WT whole skin cell suspensions without or with dispase treatment. (C) Facs dot plots of Vγ6 (17D1 mAb) staining of CD45+ live cells from uterus cell suspensions with or without dispase treatment. (D) Negative control staining with the secondary Ab (Mouse Anti-Rabbit, MAR) without 17D1 mAb (dot plots representative of 3 independent experiments).

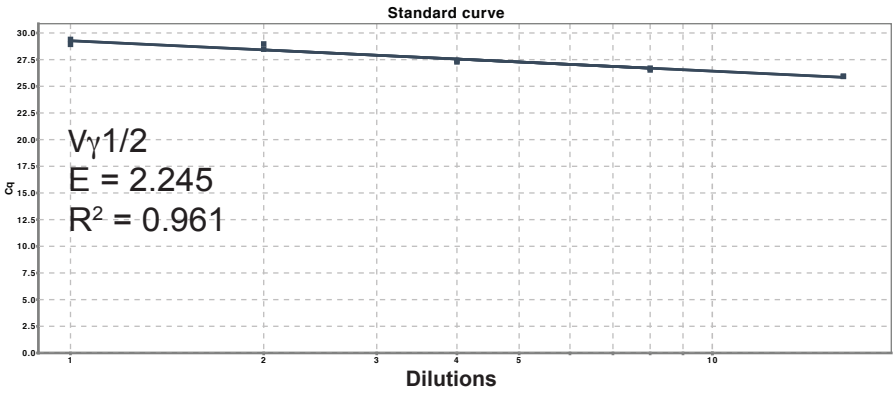

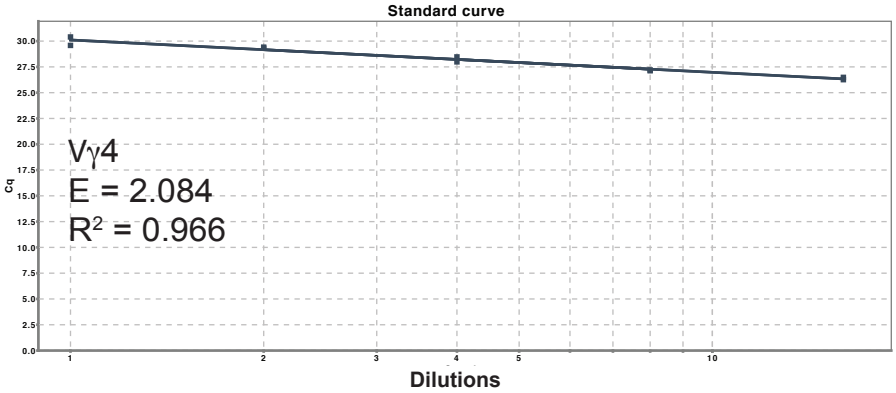

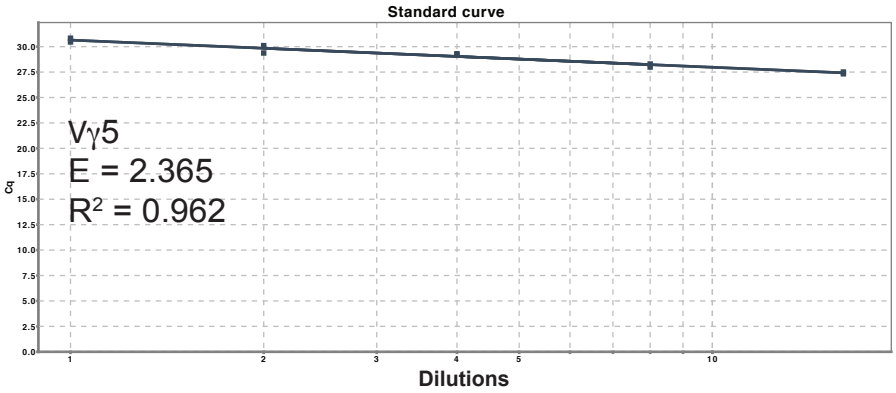

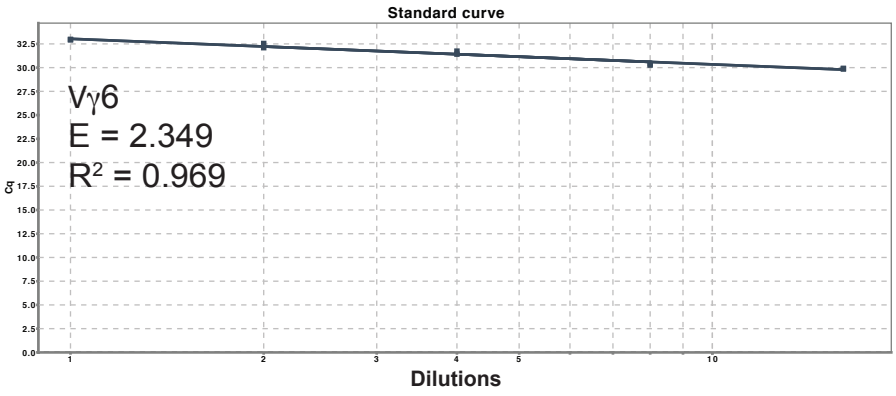

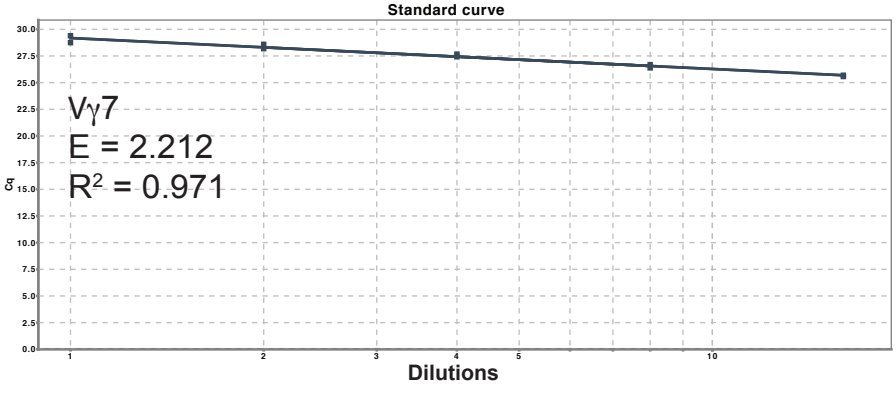

Fig. S6. Vγ chains qPCR efficacy. Serial dilutions of cDNA mix from mRNA extraction of WT mouse lymph node, uterus and intestine tissues have been used to test the PCR efficency for Vγ1/2, Vγ4, Vγ5, Vγ6, Vγ7. The efficiency is calcultated as follow: $E = 2^{(-1/slope)}$.

Figure S7

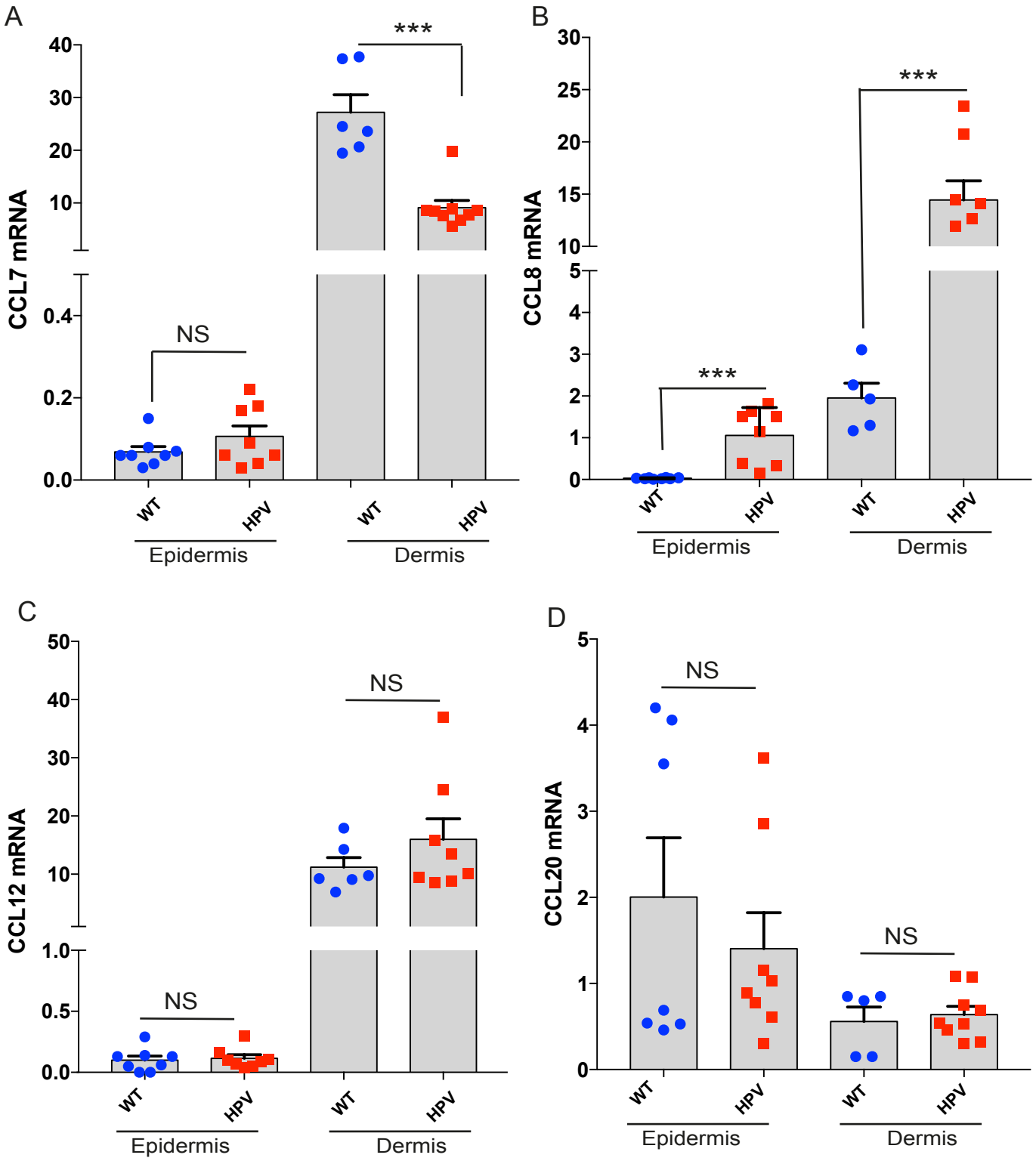

Figure S7. Expression of the CCR2 ligands CCL7 (A), CCL8 (B) and CCL12 (C) and the CCR6 ligand CCL20 (D).

mRNA levels were measured by qPCR in epidermis and dermis of week 6/7-old WT (blue circles) and HPV (red squares) mice (anova test, means + SEM, NS= non significant, *** $p<0.005$).

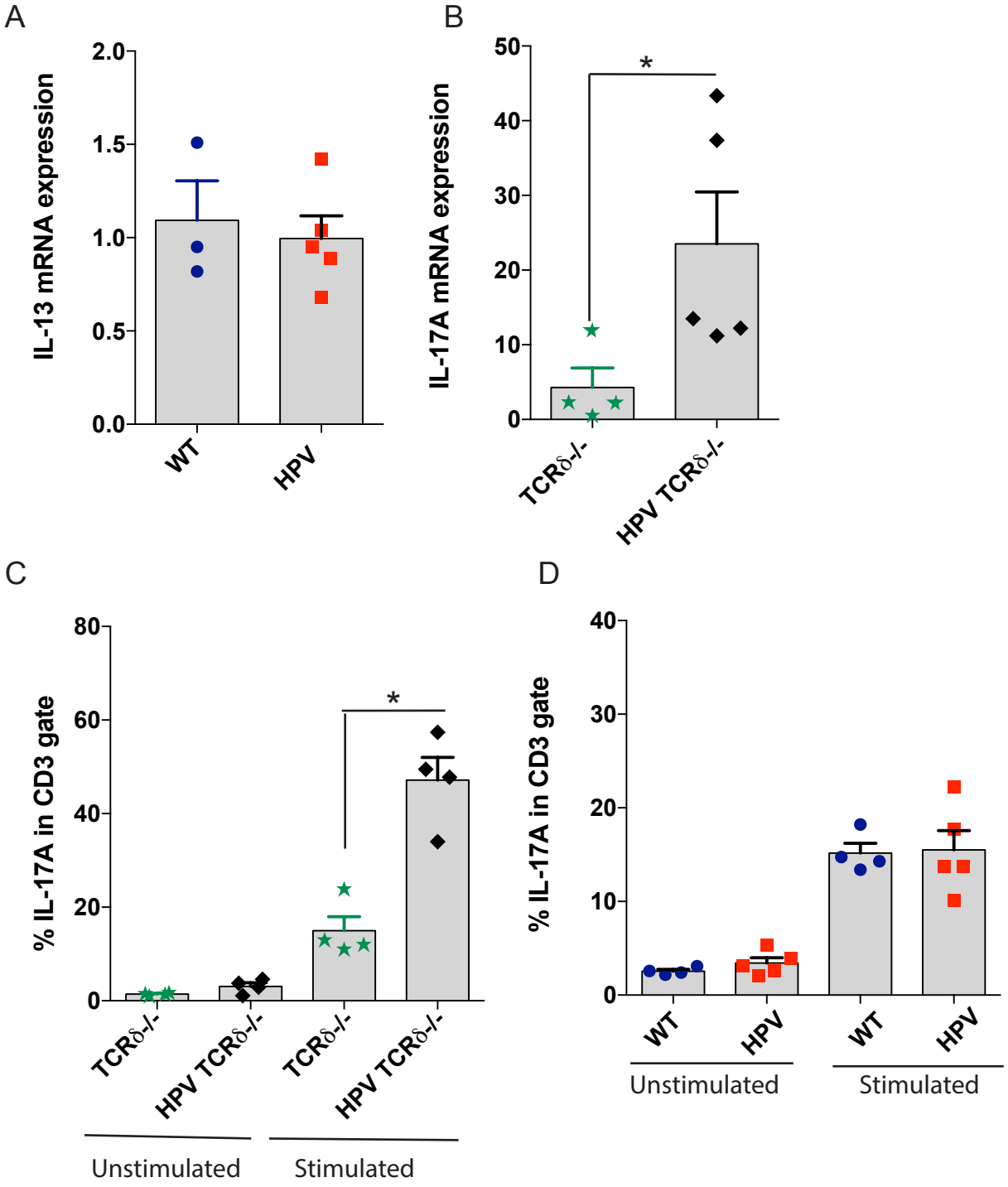

Fig. S8. IL-13 and IL-17A expression.
(A) IL-13 mRNA expression was measured by qPCR WT and HPV mouse epidermis. (B) IL-17A mRNA expression was measured by qPCR in TCRδ-/- and HPV TCRδ-/- mouse epidermis. (C) Percentages of IL-17A+ cells in CD3+ gate determined by FACS intracytoplasmic staining on cells isolated from epidermis and stimulated or not by PMA and ionomycin (Mann-Whitney test, mean + SEM, * = $p < 0.05$). (D) Percentages of IL-17A+ cells in CD3+ gate determined by FACS intracytoplasmic staining on cells isolated from dermis and stimulated or not with PMA and ionomycin (mean + SEM). All mice are 6-7 week-old.

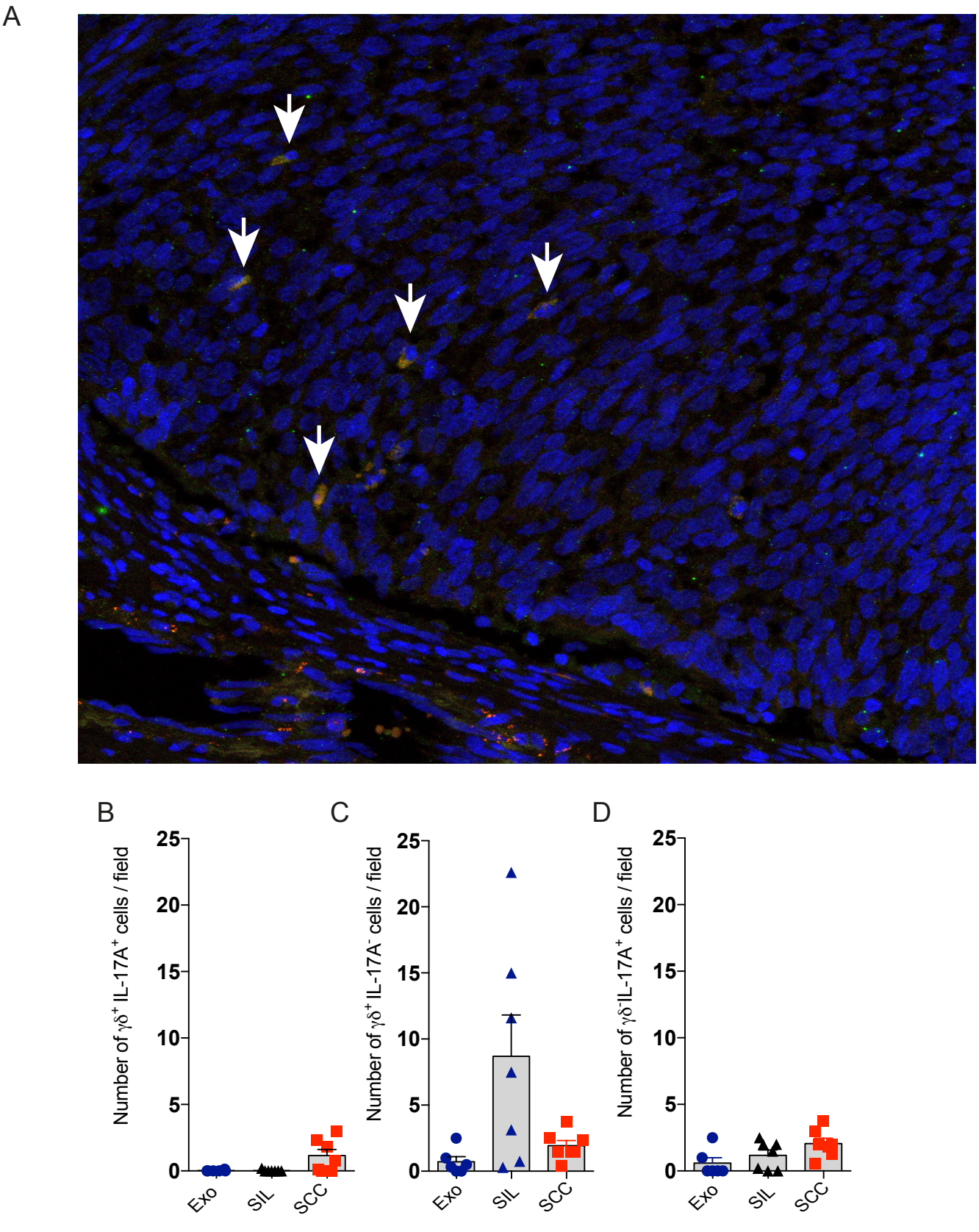

Fig. S9. IL-17A+ cells in HPV-associated lesions.
(A) γδ+ IL-17A+ cells (arrows) in SCC. (B-D) Quantification of human γδ+ IL-17A+ (B), γδ+ IL-17A- (C) and γδ- IL-17A+ (D) T cells in stroma underlying normal exocervix (Exo), preneoplasic lesions (SIL) and SCC biopsies (mean + SEM).

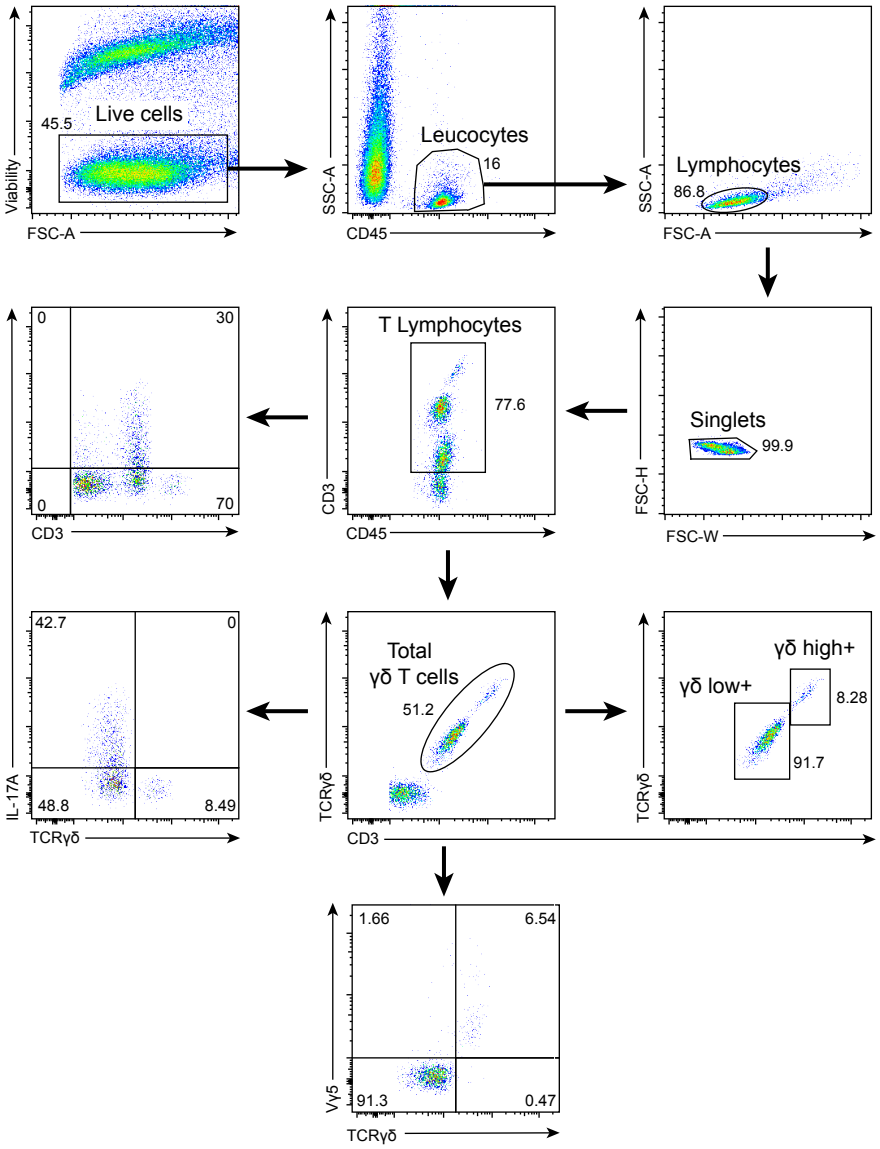

Fig. S10. Facs gating strategy.
Cells were isolated from ear epidermis of week 6-old HPV mouse.

Supplementary tables

Table S1 : Primer sequences for qPCR analysis

Primers	Sequence 5' – 3'	References
Vγ1/2 Forward	ACA CAG CTA TAC ATT GGT AC	(1)
Vγ4 Forward	TGT CCT TGC AAC CCC TAC CC	
Vγ5 Forward	TGT GCA CTG GTA CCA ACT GA	
Vγ6 Forward	GGA ATT CAA AAG AAA ACA TTG TCT	
Vγ7 Forward	AAG CTA GAG GGG TCC TCT GC	
Cγ Common Reverse	CTT ATG GAG ATT TGT TTC AGC	
IL-17A Forward	GAA GGC CCT CAG ACT ACC TC	Designed using the Primer3 program
IL-17A Reverse	CTT TCC CTC CGC ATT GAC AC	
IL-13 Forward	GCT TAT TGA GGA GCT GAG CAA CA	(2)
IL-13 Reverse	GCC AGG TCC ACA CTC CAT A	
Skint1 Forward	TTC AGA TGG TCA CAG CAA GC	(3)
Skint1 Reverse	GAA CCA GCG AAT CTC CAT GT	
Rae1 Forward	CAG GTG ACC CAG GGA AGA TG	(4)
Rae1 Reverse	CTC AAC TCC TGG CAC AAA TCG	
CCL2 Forward	TGG CTC AGC CAG ATG CAG T	(5)
CCL2 Reverse	TCT TTG GGA CAC CTG CTG CT	
CCL7 Forward	GCT GCT TTC AGC ATC CAA GTG	PrimerBank ID 7305463a1
CCL7 Reverse	CCA GGG ACA CCG ACT ACT G	
CCL8 Forward	TAA GGC TCC AGT CAC CTG CT	(6)
CCL8 Reverse	TTC CAG CTT TGG CTG TCT CT	
CCL12 Forward	ATT TCC ACA CTT CTA TGC CTC CT	PrimerBank ID6755420a1
CCL12 Reverse	ATC CAG TAT GGT CCT GAA GAT CA	
CCL20 Foward	GTG GGT TTC ACA AGA CAG ATG	(7)
CCL20 Reverse	TTT TCA CCC AGT TCT GCT TTG	
UBC Forward	AGC CCA GTG TTA CCA CCA AG	Designed using the Primer3 program
UBC Reverse	ACC CAA GAA CAA GCA CAA GG	
TBP Forward	GGC CTC TCA GAA GCA TCA CTA	Designed using the Primer3 program
TBP Reverse	GCC AAG CCC TGA GCA TAA	

Table S2 : Murine antibodies

Techniques	Immunogen	Fluorochrome	Clone
FLOW CYTOMETRY	CD16/32	Purified	2.4G2
	Pan-γδ	APC	GL3
	Vγ5	FITC	536
	Vγ5/6	Purified	17D1
	Vγ4	FITC	UC3-10A6
	CD45	BV510	30-F11
	CD3	eFluor780	17A2
	CCR2	PE	475901
	CCR6	PE	140706
	IL-17A	PE	17B7
IHC	VWF	Purified	Polyclonal
IF	Pan-γδ	Purified (Secondary coupled with AlexaFluor 568)	GL3
	Vγ5	FITC	536
	CD3	AF 488	17A2

Table S3 : Human antibodies

Techniques	Immunogen	Fluorochrome	Clone
IHC	TCR CγM1	Purified	γ3.20
	CD3		Polyclonal
IF	TCR CγM1	Purified (Secondary coupled with AlexaFluor 488)	γ3.20
	IL-17A	Purified (Secondary coupled with AlexaFluor 594)	Polyclonal

References supporting files

1. Kim JH, et al. (2016) Programmed cell death ligand 1 alleviates psoriatic inflammation by suppressing IL-17A production from programmed cell death 1-high T cells. *J Allergy Clin Immunol* 137(5):1466–1476.

2. Dalessandri T, Crawford G, Hayes M, Castro Seoane R, Strid J (2016) IL-13 from intraepithelial lymphocytes regulates tissue homeostasis and protects against carcinogenesis in the skin. *Nat Commun* 7:12080.

3. Roberts NA, et al. (2012) Rank signaling links the development of invariant γδ T cell progenitors and Aire(+) medullary epithelium. *Immunity* 36(3):427–437.

4. Jung H, Hsiung B, Pestal K, Procyk E, Raulet DH (2012) RAE-1 ligands for the NKG2D receptor are regulated by E2F transcription factors, which control cell cycle entry. *J Exp Med* 209(13):2409–2422.

5. Ramírez-Valle F, Gray EE, Cyster JG (2015) Inflammation induces dermal Vγ4+ γδT17 memory-like cells that travel to distant skin and accelerate secondary IL-17-driven responses. *Proc Natl Acad Sci USA* 112(26):8046–8051.

6. Severa M, et al. (2014) The Transcriptional Repressor BLIMP1 Curbs Host Defenses by Suppressing Expression of the Chemokine CCL8. *J Immunol* 192(5):2291–2304.

7. Kao C-Y, et al. (2005) Up-regulation of CC chemokine ligand 20 expression in human airway epithelium by IL-17 through a JAK-independent but MEK/NF-kappaB-dependent signaling pathway. *J Immunol* 175(10):6676–6685.